An Aggregated Approach to Harmonic Modelling of Loads in Power Distribution Networks

Möllerstedt, Erik

1998

Document Version:
Publisher's PDF, also known as Version of record

An Aggregated Approach to Harmonic Modelling of Loads in Power Distribution Networks

Erik Möllerstedt

Department of Automatic Control
Lund Institute of Technology
Lund, June 1998

Department of Automatic Control
Lund Institute of Technology
Box 118
S-221 00 LUND
Sweden

ISSN 0280–5316
ISRN LUTFD2/TFRT–3221–SE

Printed in Sweden by Reprocentralen, Lunds Universitet.
Lund 1998

Contents

Acknowledgments

Among the people that I would like to thank are my supervisors, Sven Erik Mattsson and Bo Bernhardsson. You have always been very helpful and enthusiastic. Olof Samuelsson has been, and will hopefully continue to be, an invaluable link to the unknown field of power systems. Thanks for all material, and also for your careful reading of the manuscript. I would also like to thank Mats Alaküla and Magnus Akke for helping me with the experiments.

The work has been supported by Elforsk, Nutek, and ABB, as Elektra project 3153. This project was recently extended another 2.5 years, for which I am very grateful. I also would like to express my gratitude to Daniel Karlsson, and Anders Åberg in the project reference group, who have come with many valuable remarks.

My friend and very good office mate Johan Christer Eker, thanks for welcoming me with a happy smile every morning. Finally, Anna, what would I do without your neverending patience and support, and Hugo, I am really sorry about all the hockey games we have had to do without....

Erik Möllerstedt

1

Introduction

During the past few decades, there has been a dramatic increase in the number of electronic devices that are connected to the power networks. Computers, TV sets, and low energy lighting are significant residential loads. Power electronics is also successfully used to control industrial loads, like adjustable speed drives. These devices distort the wave form of current and voltage of the supplied power.

While the power becomes more distorted, society becomes more dependent on a supply of power of good quality. Power distortion leads to increased losses and overheating of components and cables that reduces the capacity of the networks. It may also result in failure of sensitive equipment.

Fortunately, power electronics also provides possibilities for more sophisticated control of the networks. Active filters, thyristor controlled series capacitors and shunt reactors, HVDC converters, and battery chargers for electric vehicles can all be controlled to improve the power quality. In order to exploit these new opportunities, there is a need for model structures that not only result in efficient simulation, but also are suitable for analysis and control design.

A major problem when modelling, analyzing and simulating distribution networks is the huge number of components. Methods to reduce the resulting large and complex models are necessary. Model reduction of linear networks is straightforward, but for nonlinear networks analytical solutions can often not be obtained.

This thesis presents an aggregated approach to modelling of nonlinear and switching loads for steady state harmonic analysis. It is a

frequency domain method, with roots in the method of harmonic balance. The models, called Harmonic Norton Equivalents, are linearized descriptions around the nominal voltage. The result is a linear relationship between the deviations in the Fourier coefficients of the current and the voltage. The linearization is justified by strict standards that limits the allowed voltage distortion in distribution networks.

The linearization implies that aggregation of models and network solving is a non-iterative procedure, using linear algebra. The model structure can be interpreted as an extension of the Norton equivalent for linear subnetworks. It facilitates a compact way to represent the behaviour of a large nonlinear and switching network and it can be obtained through simple experiments avoiding detailed modelling.

The structure of the Harmonic Norton Equivalents has been developed for the purpose of analyzing nonlinear and switching networks, with respect to harmonic contents, periodic stability, and robustness. They can also be used for improved load representation in time domain simulation programs. Furthermore, existing model libraries from time domain simulation programs can be used to obtain the equivalents, which means that frequency domain modelling of nonlinear and switching loads is not necessary.

1.1 Outline of the Thesis

In Chapter 2 some background to computer simulation of power networks is given. The nodal formulation is shown to be suitable way for getting a mathematical model for a network in an automatized way. It is described how the nodal formulation is solved by dominating simulation programs. Finally, it is shown how the special structure of periodic signals can be used to solve nonlinear networks in steady state.
In Chapter 3 the Harmonic Norton Equivalent is presented. The model for a light dimmer, is validated and shown to be suitable for analysis of distribution network under normal operation. It is also shown how aggregation of Harmonic Norton Equivalents and network solving is performed.
In Chapter 4 a procedure is presented for obtaining Harmonic Norton Equivalents from measurements or time domain simulation.

2

Power Network Simulation

Power systems are very complex, they are widespread and contain numerous components: lines, cables, generators, transformers and switch yards, protective equipment like breakers and surge arresters, and control equipment such as capacitor banks, static var compensators, and power system stabilizers. An enormous amount of different electric loads are connetcted to the network. Computer methods for analysis and simulation have been used in power system design for a long time, as large scale experiments for security and economical reasons can be performed only to a very limited extent.

Dominating programs for simulation of electric power networks, like EMTP, are not designed for efficient simulation of networks that contain a lot of switching electronic components. However, the strength of these programs is their widespread use and the vast and thoroughly validated model libraries, and they will continue to be the dominating programs for a long time. Any method for analysis and simulation of switching systems ought for this reason be developed for use in combination with these programs.

In this chapter it is shown how nodal analysis is used to obtain mathematical models of electrical networks. Nodal analysis facilitates a simple way to get the models from graphical inputs, which is used by modern simulation tools to automatize the modelling. It is also shown how programs like EMTP solve the network equations. Finally, the method of harmonic balance is described as a powerful way to derive the steady state solution of networks with nonlinear and switching components.

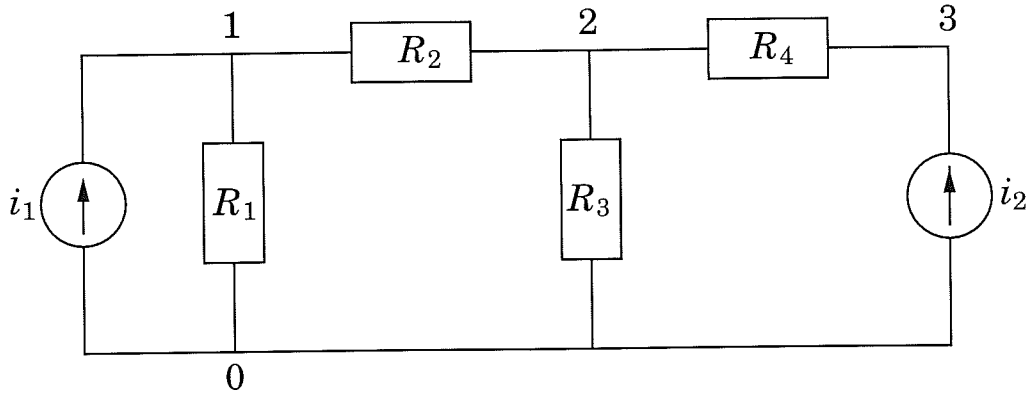

Figure 2.1 A small network with four resistors and two current sources.

2.1 The Nodal Formulation

A mathematical model of an electric network is conveniently obtained by nodal analysis [Vlach and Singhal, 1994]. Kirchhoff's current law (KCL), which states that the sum of the currents that flow into each node is zero, is used for every node of the system to describe the relationship between the node voltages.

As an example, the node equations for the network in Figure 2.1 are obtained using KCL for the three nodes, 1–3

$$\begin{cases} i_1 - \frac{1}{R_1}v_1 - \frac{1}{R_2}(v_1 - v_2) = 0, \\ \frac{1}{R_2}(v_1 - v_2) - \frac{1}{R_3}v_2 - \frac{1}{R_4}(v_2 - v_3) = 0, \\ \frac{1}{R_4}(v_2 - v_3) + i_2 = 0. \end{cases}$$

The equation for node 0, the reference node, is left out to avoid an over-determined system. The system can be rewritten to get the nodal formulation

$$\begin{bmatrix} \frac{1}{R_1} + \frac{1}{R_2} & -\frac{1}{R_2} & 0 \\ -\frac{1}{R_2} & \frac{1}{R_2} + \frac{1}{R_3} + \frac{1}{R_4} & -\frac{1}{R_4} \\ 0 & -\frac{1}{R_4} & \frac{1}{R_4} \end{bmatrix} \begin{bmatrix} v_1(t) \\ v_2(t) \\ v_3(t) \end{bmatrix} = \begin{bmatrix} i_1(t) \\ 0 \\ i_2(t) \end{bmatrix}.$$

The nodal formulation allows all linear resistive networks to be described by a linear equation system

$$\mathcal{Y}\mathcal{V}(t) = I(t), \tag{2.1}$$

where $\mathcal{V}(t)$ is a vector containing the node voltages, $I(t)$ contains the external current sources, and the admittance matrix $\mathcal{Y}$ is a matrix built up by the resistive elements in the network.

To fit the nodal formulation, external voltage sources are transformed to Norton equivalents. A Norton equivalent consists of a current source and an impedance in parallel, and can be used to describe the behaviour of any linear subnetwork as seen from two terminals.

The nodal formulation for a network can be obtained directly from the network topology. The diagonal element Y_{ii} of the admittance matrix is the sum of the admittances connected to node i. The off-diagonal element Y_{ij} is the admittance connected between nodes i and j with negative sign. Modern modelling tools use this structure to obtain a mathematical model of a network from graphical inputs. It is easy to add or remove components, even if this results in a changed topology for the network. This is the reason for the popularity of the nodal formulation for computer analysis of electrical networks, even if other approaches may result in more efficient simulation.

2.2 Solving the Network

The node voltages of a resistive network are obtained by solving the linear algebraic equation system (2.1). If the network contains dynamic elements, like capacitors and inductors, network solving is more involved. The nodal formulation (2.1) is then a differential-algebraic equation system (DAE-system).

Capacitive components can be included in the nodal formulation by allowing the elements of the admittance matrix to include the differential operator. A linear capacitor is described by

$$C\frac{dv}{dt} = i.$$

The admittance for a capacitor is thus

$$Y_C = C\frac{d}{dt},$$

or by using Laplace transforms

$$Y_C = Cs.$$

For inductors, the relation between current and voltage is

$$L\frac{di}{dt} = v.$$

To include inductive components, the nodal formulation must be modified to allow branch currents in the state vector.

Network Solving in EMTP

EMTP (Electro Magnetic Transients Program) [EPRI, 1989] is, together with some closely related programs like ATP and EMTDC, the dominating program for analysis of electro-magnetic transients in power systems. It was developed in the late 1960's by Hermann Dommel at Bonneville Power Administration.

The power of EMTP is the extensive model libraries, with thoroughly validated models for machines, transformers, cables, and transmission lines. EMTP has been an industrial standard for a long time, and has been used for numerous benchmark problems.

EMTP uses a simple approach to simulate the DAE-system. Each time step, the dynamical components are integrated using the trapezoidal rule. For a capacitor this gives

$$C\frac{v(t) - v(t - \Delta t)}{\Delta t} = \frac{i(t) + i(t - \Delta t)}{2},$$

which gives for the current

$$i(t) = \frac{2C}{\Delta t}v(t) + I(t - \Delta t),$$

where

$$I(t - \Delta t) = -i(t - \Delta t) - \frac{2C}{\Delta t}v(t - \Delta t).$$

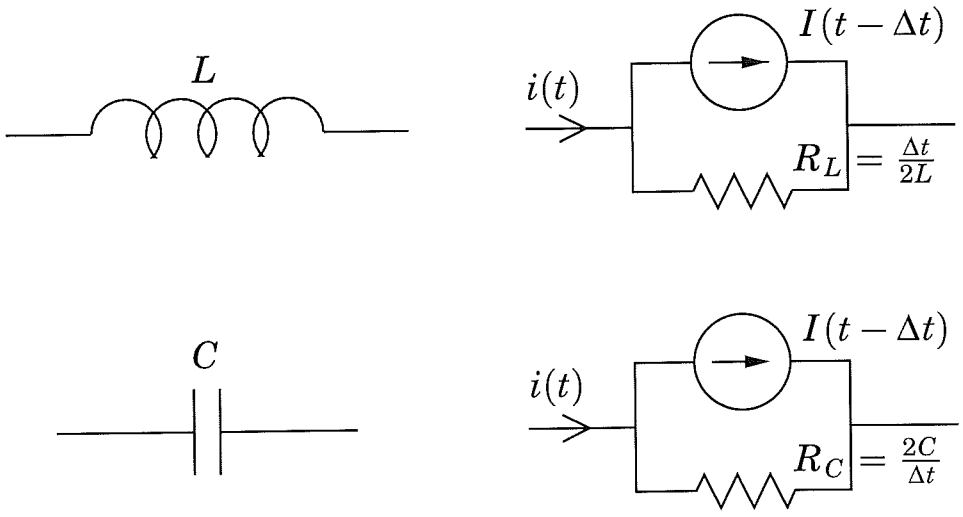

Figure 2.2 Using the trapezoidal rule for integration, dynamic elements like inductors and capacitors can be treated as resistors in parallel with a current source.

This way, the capacitor can be interpreted as a resistor in parallel with a current source, which serves as the memory of the dynamics, see Figure 2.2. Similarly, an inductor is described by

$$i(t) = \frac{\Delta t}{2L} v(t) + I(t - \Delta t),$$

where

$$I(t - \Delta t) = i(t - \Delta t) + \frac{\Delta t}{2L} v(t - \Delta t).$$

These models for the capacitor and the inductor are called companion models.

Using companion models, the network becomes resistive. Every time step, the current sources for the companion models are updated, and then the resistive network is solved. A fixed time step is used, which means that the resistors in the network are constant throughout the simulation, and only the current sources are updated. The same LU-factorization can be used for the whole simulation.

Nonlinear and Switching Loads

Nonlinear and switching devices do not fit in the nodal formulation. In EMTP, nonlinear loads and control systems are treated as current

sources. Every time step the linear part of the network is solved, and then the current sources are updated with respect to the new node voltages. The updating is performed by a separate simulation program, called TACS (Transient Analysis of Control Systems), run in parallel with EMTP. The separation of the system in a linear and a nonlinear part implies that a delay of one time step is introduced. For slow dynamics, it may not be so severe, but for systems including switchings and sharp nonlinearities, it is important to determine the switching instants accurately. Thus very short time steps are required, which leads to inefficient simulation.

For simulation of systems with multiple switchings, for instance converter stations in HVDC networks, there is a need for some way to allow more than one switching action at each time step. To accomplish this, the whole switching sequence must be modelled in TACS. This might be easy to do under normal working conditions, but it is hard to foresee the switching sequence during a disturbance.

The trapezoidal rule is not good for simulation of switching systems, as it leads to numerical oscillations [Mohan *et al.*, 1994]. One way to avoid numerical oscillations is to use a more stable method for the integration steps following every switch. The Critical Damping Adjustment (CDA) implemented in DCG/EPRI EMTP Version 3 uses the more stable backward Euler integration method for two half time steps after every switch. The closely related simulation software EMTDC, developed by Manitoba Hydro and Manitoba HVDC Research Center especially for HVDC-studies uses interpolation to avoid numerical oscillations. The use of interpolation gives the correct switching instants and simplifies the treatment of multiple switchings. This makes EMTDC more suitable for power electronics modelling and simulation.

2.3 Steady State Simulation

Programs like EMTP were originally designed for transient studies, including line faults, load losses, and lightning phenomena. However, these programs are frequently used for steady state analysis too. There are a few problems with this. Networks with switching components are, so called, stiff systems, with both fast and slow dynamics. The slow dynamics imply that the system has to be simulated for a long

time until it reaches steady state, whereas the fast dynamics require a very short time step. The resulting simulation work is large. It might also be hard to tell whether the system has actually reached steady state.

Representation of Periodic Signals

A network is said to be in steady state if all currents and voltages are periodic with period T. This periodic nature of the signals can be used to obtain efficient methods for network solving in frequency domain. Periodic signals are well approximated by truncated Fourier series

$$i(t) = \sum_{k=-N}^{N} C_k e^{jk\omega_0 t},$$

$$v(t) = \sum_{k=-N}^{N} c_k e^{jk\omega_0 t},$$

where $\omega_0 T = 2\pi$.

Let the current spectrum, I, and the voltage spectrum, V, be complex vectors containing the Fourier coefficients of source current and node voltage respectively,

$$I = [\, C_{-N} \quad C_{-N+1} \quad \dots \quad C_{-1} \quad C_0 \quad C_1 \quad \dots \quad C_{N-1} \quad C_N \,]^T,$$

$$V = [\, c_{-N} \quad c_{-N+1} \quad \dots \quad c_{-1} \quad c_0 \quad c_1 \quad \dots \quad c_{N-1} \quad c_N \,]^T.$$

For linear components, there is a linear relation between the current spectrum and the voltage spectrum

$$I = YV, \tag{2.2}$$

where Y is a matrix of size $(2N+1) \times (2N+1)$. For a resistor, an inductor, and a capacitor, the Y-matrices are

$$Y_R = \mathrm{diag}(\frac{1}{R}, \frac{1}{R}, \dots, \frac{1}{R}),$$

$$Y_L = \mathrm{diag}(-\frac{1}{jN\omega_0 L}, -\frac{1}{j(N-1)\omega_0 L}, \dots, \frac{1}{jN\omega_0 L}),$$

$$Y_C = \mathrm{diag}(-jN\omega_0 C, -j(N-1)\omega_0 C, \dots, jN\omega_0 C),$$

respectively, with ω_0 denoting the fundamental frequency. The matrices are diagonal, which means that there is no coupling between different frequencies. This is due to the linearity of the components.

Assuming periodic signals, the time domain equation system in Equation (2.1) is transformed to a relation between the spectra, I_i and V_i. The solution for the linear network is obtained from the linear algebraic equation system

$$\underbrace{\begin{bmatrix} Y_1+Y_2 & \vdots & -Y_2 & \vdots & 0 \\ \cdots & \cdots & \cdots & \cdots & \cdots \\ -Y_2 & \vdots & Y_2+Y_3+Y_4 & \vdots & -Y_4 \\ \cdots & \cdots & \cdots & \cdots & \cdots \\ 0 & \vdots & -Y_4 & \vdots & Y_4 \end{bmatrix}}_{\mathcal{Y}} \underbrace{\begin{bmatrix} V_1 \\ \cdots \\ V_2 \\ \cdots \\ V_3 \end{bmatrix}}_{\mathcal{V}} = \underbrace{\begin{bmatrix} I_1 \\ \cdots \\ 0 \\ \cdots \\ I_2 \end{bmatrix}}_{I}.$$

The size of the equation system is $M(2N+1)$, where M is the number of nodes in the network.

As the admittance matrices are diagonal, the different frequencies are uncoupled, and can be solved for separately. Instead of solving a system of $M(2N+1)$ equations, it is sufficient to solve $2N+1$ different systems with M equations each.

Linear dynamic components, like inductors and capacitors, make network solving in time domain much more involved compared to a purely resistive network. In frequency domain, dynamic components do not cause any problems. As only the steady state solution is wanted, dynamic components can be treated in the same way as static ones. In frequency domain, the DAE-system in Equation (2.1) is transformed to a linear algebraic equation system, even if the network has dynamic components.

Trigonometric Fourier Series

To avoid complex numbers and negative frequencies, the trigonometric

Fourier series can be used

$$i(t) = \sum_{k=1}^{N} A_k \cos k\omega_0 t + B_k \sin k\omega_0 t,$$
$$v(t) = \sum_{k=1}^{N} a_k \cos k\omega_0 t + b_k \sin k\omega_0 t,$$

with spectra

$$I = [A_1 \quad B_1 \quad \dots \quad A_N \quad B_N]^T,$$
$$V = [a_1 \quad b_1 \quad \dots \quad a_N \quad b_N]^T.$$

Using the trigonometric Fourier series, the admittance matrix for a resistor is still diagonal, but for an inductor and a capacitor the admittance matrices becomes block diagonal

$$Y_L = \text{diag}\left(\frac{1}{\omega_0 L}\begin{bmatrix}0 & -1\\ 1 & 0\end{bmatrix}, \frac{1}{2\omega_0 L}\begin{bmatrix}0 & -1\\ 1 & 0\end{bmatrix}, \dots, \frac{1}{N\omega_0 L}\begin{bmatrix}0 & -1\\ 1 & 0\end{bmatrix}\right),$$
$$Y_C = \text{diag}\left(\omega_0 C\begin{bmatrix}0 & 1\\ -1 & 0\end{bmatrix}, 2\omega_0 C\begin{bmatrix}0 & 1\\ -1 & 0\end{bmatrix}, \dots, N\omega_0 C\begin{bmatrix}0 & 1\\ -1 & 0\end{bmatrix}\right).$$

2.4 Harmonic Balance

For nonlinear and switching devices, the relation between I and V in Equation (2.2) becomes nonlinear. This means that the network no longer can be solved by LU-factorization. One way of solving nonlinear networks is the method of harmonic balance. In harmonic balance, the network is split into two parts, a linear network, and a collection of nonlinear components. The currents through the nonlinear components are derived with respect to the node voltages, and the linear network is solved as described in the previous section, with the nonlinear components treated as harmonic current sources.

The resulting equation to be solved is the nonlinear equation

$$F(\mathcal{V}) = \mathcal{Y}\mathcal{V} - I(\mathcal{V}) = 0, \tag{2.3}$$

where $\mathcal{Y}$ is the admittance matrix from the linear part of the network, $\mathcal{V}$ is a large vector built up by the voltage spectrum vectors, V_i, at every node, and $I(\mathcal{V})$ is built up by the current spectrum vectors of all external sources and nonlinear loads.

The nonlinear algebraic equation system, (2.3), can be solved in a number of ways. In [Kundert and Sangiovanni-Vincentelli, 1986] and [Gilmore and Steer, 1991], three different approaches are discussed, namely optimization methods, relaxation methods, and Newton's method.

Optimization Methods

The optimization methods use an optimizer to find the voltage vector $\mathcal{V}$ that minimizes the quadratic error function $\varepsilon(\mathcal{V}) = F(\mathcal{V})^* F(\mathcal{V})$ where the asterisk denotes conjugate transpose. The optimal $\mathcal{V}$ is the least squares minimum of Equation (2.3). Most often, some quasi-Newton method is used. Optimization is hard because of the large number of variables and equations. When forming the error function, all errors are added up and information about signs and location of the errors in the network is lost.

Relaxation Methods

In relaxation methods, the network equation is solved iteratively

$$\mathcal{Y}\mathcal{V}^{(j+1)} = I(\mathcal{V}^{(j)}).$$

The node voltages from the j'th iteration are used to calculate the currents from the nonlinear components for the next iteration. This way, the network equation is kept linear, and can be solved frequency by frequency. The result is a fast method with little memory usage. The method works well for small, near linear networks, but for large networks, with many nonlinear components, many iterations are needed. Even with good initial values, convergence cannot be guaranteed.

Newton's Method

Newton's method applied to Equation (2.3) leads to the following iterative scheme

$$\mathcal{V}^{(j+1)} = \mathcal{V}^{(j)} - J(\mathcal{V}^{(j)})^{-1} F(\mathcal{V}^{(j)}),$$

where

$$J(\mathcal{V}) = \frac{dF}{d\mathcal{V}} = \mathcal{Y} + \frac{dI(\mathcal{V})}{d\mathcal{V}} \tag{2.4}$$

is the Jacobian of $F(\mathcal{V})$. The Jacobian is not diagonal, and the off-diagonal elements define the coupling between different frequencies. This means that the different frequencies cannot be solved for separately. For large networks with many harmonics considered, the required memory and the computational effort are large. The convergence for Newton's method is superior to the one for the relaxation methods. With good initial conditions, Newton's method has quadratic convergence. For networks with many and strongly nonlinear components, the reduction in the number of iterations required may well motivate the extra work at each iteration.

The computational work can be reduced by using the same Jacobian for several iterations. This results in an increase of the number of iterations required, but the total computational effort is often reduced.

Another way to reduce the computational work can be applied to networks with soft nonlinearities, that is almost linear components where the coupling between different frequencies is weak. For these components, the admittance matrix, Y, is almost diagonal. By setting all off-diagonal elements to zero, the different frequencies remain decoupled, and it is not necessary to solve for all harmonics simultaneously. This, in combination with not having to do time consuming Jacobian calculations can lead to faster and more robust network solving.

Harmonic Balance and Power Networks

The method of harmonic balance has been applied to power networks under various names. Newton's method of harmonic balance is called *Harmonic Power Flow Study* in [Xia and Heydt, 1982], it is called *Unified Solution of Newton Type* in [Acha *et al.*, 1989], and *Harmonic Domain Algorithm* in [Arrillaga *et al.*, 1994]. Harmonic balance with relaxation is called *Iterative Harmonic Analysis* in [Arrillaga *et al.*, 1987], and Newton's method with a diagonal Jacobian is called *A Multiphase Harmonic Load Flow Solution Technique* in [Xu *et al.*, 1991].

Component Models

An important step in the method of harmonic balance is to calculate the current through the nonlinear components for a known voltage, that is the function $I(\mathcal{V})$ in Equation 2.3. A problem is that there is often no convenient way to represent the nonlinear components in frequency domain. In this case, the nonlinear components have to be simulated in time domain, using as input a time domain signal reconstructed from the Fourier coefficients of node voltages and the Fourier coefficients of the current are then obtained via FFT. This is particularly problematic for the optimization methods, where numerous different operating points must be evaluated. For Newton's method, time domain models for the nonlinear components imply that the Jacobian has to be derived numerically. For efficiency and robustness, frequency domain models must be used.

Frequency domain modelling of nonlinear and switching components is often quite involved, and many papers have been written about modelling of special components like transformers with nonlinear saturation curves [Semlyen *et al.*, 1988; Semlyen and Rajaković, 1989; Acha *et al.*, 1989], HVDC converters [Song *et al.*, 1984; Arrillaga and Callaghan, 1991; Xu *et al.*, 1994] and static var compensators [Xu *et al.*, 1991].

Harmonic Balance and Distribution Networks

The method of harmonic balance is efficient for analysis of large network with a few nonlinear components. The linear parts are aggregated to small equivalents, which reduces the size of the models. For distribution networks with numerous nonlinear and switching loads, it is necessary to aggregate nonlinear components, and also to obtain models for aggregated loads without detailed modelling.

2.5 The Goal of Harmonic Studies

In [Ranade and Xu, 1998] the authors state that the goal of harmonic studies is to quantify the distortions in voltage and current waveforms at various points in a power system. Harmonic studies can also determine the existence of dangerous resonant conditions and verify com-

pliance with harmonic limits. The harmonic study consists of the following steps:

- Definition of harmonic-producing equipment and determination of models for their representation.
- Determination of the models to represent other components in the system including external networks.
- Simulation of the system for various scenarios.

With the possibilities for more sophisticated control of the networks, which have been accomplished with the use of power electronics, the goals of harmonic studies must be extended. As efficient control increases the capacity of the network, the stability margins are tightened. There is a need for robustness analysis that can tell not only whether dangerous resonant conditions exist or harmonic limits are exceeded, but also how close to such undesired states the system is. When modelling networks, the goal should not only be efficient simulation, but also models that can be used for analysis and control design.

3

Harmonic Norton Equivalents

In this chapter a model structure for nonlinear and switching loads in distribution networks is presented. The models define an affine relation between the Fourier coefficients of the voltage and the current. The models are valid for steady state analysis.

The models facilitate a straightforward way of aggregating nonlinear loads. It is a modularized approach to network analysis. A major advantage with the models is that aggregated loads can be obtained numerically from measurements or time domain simulation. This means that detailed, often impossible, modelling work is avoided.

3.1 The Model Structure

For steady state analysis, periodic signals can be described by Fourier series, as stated in Section 2.3. The trigonometric Fourier series is used to avoid complex differentiation, which is complicated, if possible at all. Furthermore, as all signals are real, it is more intuitive to work with real numbers and positive frequencies. The advantage with the complex Fourier series, that it gives diagonal admittance matrices, is lost when modelling nonlinear components.

To fit the nodal formulation, nonlinear components must be described as current sources. Therefore, it is desirable to have an explicit expression for the current as a function of the voltage. If only small

deviations of the voltage are considered, this dependence between the Fourier vectors of the current and the voltage

$$I = [A_1 \quad B_1 \quad \dots \quad A_N \quad B_N]^T,$$
$$V = [a_1 \quad b_1 \quad \dots \quad a_N \quad b_N]^T,$$

is approximately linear. This observation leads to the following linearized model structure

$$I = I_0 + Y(V - V_0), \tag{3.1}$$

where I_0, the nominal Fourier vector of the current, describes the current at nominal voltage, with Fourier vector V_0.

The admittance matrix Y describes how the current spectrum is affected by changes in the voltage spectrum. Each column in Y describes the change in the current spectrum when a small cosine or sine component of a certain harmonic frequency is added to the nominal voltage,

$$Y = \frac{\partial I}{\partial V} = \begin{bmatrix} \frac{\partial A_1}{\partial a_1} & \frac{\partial A_1}{\partial b_1} & \cdots & \frac{\partial A_1}{\partial b_N} \\ \frac{\partial B_1}{\partial a_1} & \frac{\partial B_1}{\partial b_1} & \cdots & \frac{\partial B_1}{\partial b_N} \\ \vdots & \vdots & \ddots & \vdots \\ \frac{\partial B_N}{\partial a_1} & \frac{\partial B_N}{\partial b_1} & \cdots & \frac{\partial B_N}{\partial b_N} \end{bmatrix}.$$

Solving the network using these linearized models can be seen as one iteration of Newton's method of Harmonic Balance, with a natural choice of initial values. The Jacobian is built up by admittance matrices, like Y in Equation 3.1. The admittance matrices are fixed and do not depend on the network configuration. The network can thus be solved by successively aggregating the components. The Jacobians can be precalculated or measured. This supports an object oriented approach to network analysis, where model libraries can be composed for reuse of aggregated load models.

A Norton Equivalent Interpretation

In Figure 3.1 it is shown how the models can be interpreted as Norton Equivalents, that is, an admittance in parallel with a current source.

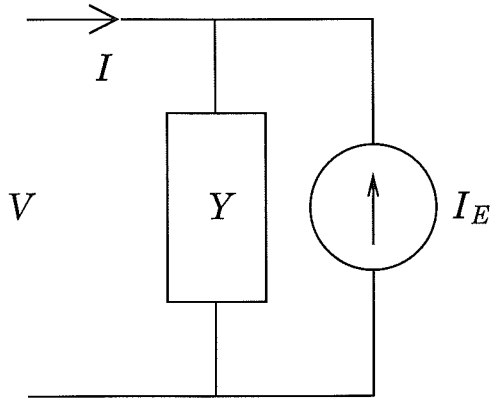

Figure 3.1 The model can be interpreted as a Norton equivalent, with an admittance matrix, Y, and a current source, I_E.

The admittance is replaced by an admittance matrix, Y, and the harmonic current source, I_E, is defined as

$$I_E = YV_0 - I_0.$$

The current I through the component is given as an affine function of the voltage

$$I = YV - I_E.$$

Because of the structure, frequency domain models used with Newton's method of harmonic balance have often been referred to as Harmonic Norton Equivalents, [Xu *et al.*, 1991; Acha *et al.*, 1989].

The powerful property of the traditional Norton equivalent, however, is not its structure, but the fact that a simple model can equivalently describe the performance of a large linear network.

The proposed model structure facilitates a simple way to aggregate components for model reduction, which allows large networks at steady state to be equivalently described by simple models. These models can be estimated by means of simple experiments with measurements or by time domain simulation, as described in Chapter 4. This way, detailed modelling of large networks is avoided. The name Harmonic Norton Equivalent is thus motivated.

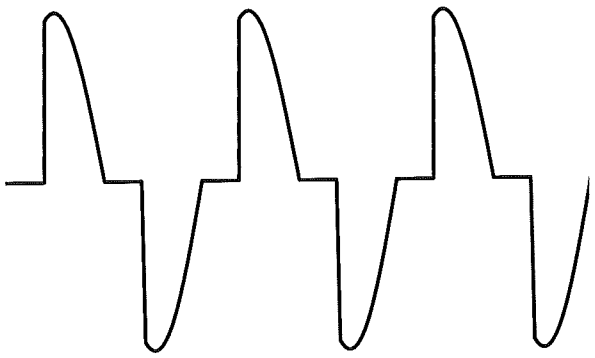

Figure 3.2 The current through a dimmer in series with a resistive load. The dimmer is turned off for a time, d, after every zero-crossing of the voltage.

3.2 Validation of the Linear Structure

As all linearized models are accurate only in a neighbourhood of the linearization point, it is of interest how large this neighbourhood is for typical components.

A Model for the Dimmer

A dimmer is investigated to get an indication of the accuracy of the model structure. The dimmer is a power electronic device used to limit the power and thus dim the light from a light bulb. The current through a dimmer is shown in Figure 3.2. The current works as an open circuit for a part of each period, and thus blocks the current through the lamp. The rest of the period, it works as a short circuit.

The harmonic spectrum of the current is shown in Figure 3.3. The switching nature of the dimmer implies that there is a sharp discontinuity in the current, which results in high distortion also at high frequencies. The dimmer constitutes a good test device. It is simple, but still has the problems associated with modelling and simulation of power electronics. The dimmer is further described in Appendix A, where also its Harmonic Norton Equivalent is derived.

It is shown in Figures 3.2 and 3.3 that the current is symmetric and the spectrum contains thus only odd harmonics. This is because the dimmer reacts identically on positive and negative voltages. As most

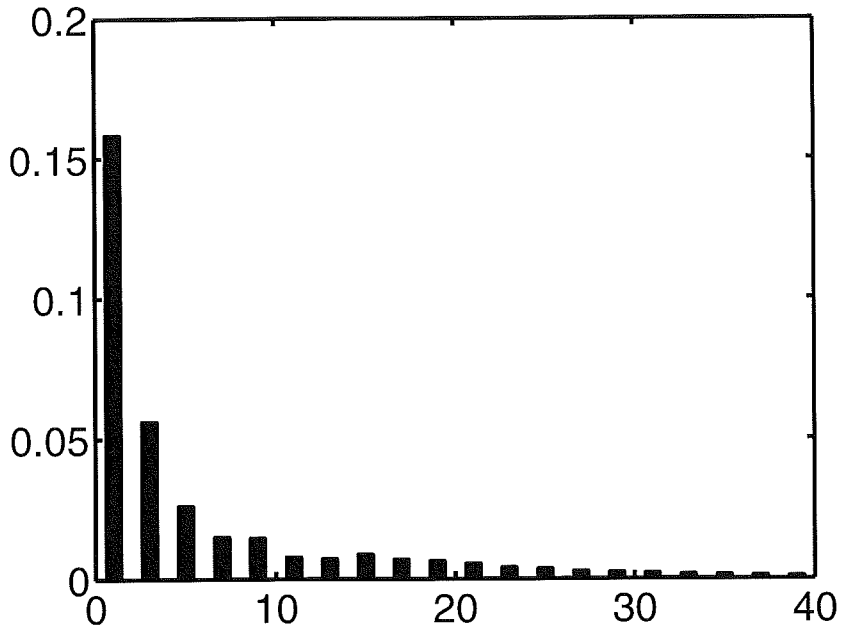

Figure 3.3 A typical current spectrum for the dimmer. As the dimmer is symmetric, there are only odd harmonics. The fundamental frequency is dominating, but the spectrum has considerable amplitudes also for high frequencies.

electrical components are symmetric, it is often enough to consider only odd harmonics. To limit the size of the models, only odd harmonics are considered in the derivation of the Harmonic Norton Equivalent for the dimmer.

To validate the Harmonic Norton Equivalent for the dimmer, it is investigated how a distortion in the voltage affects the current. For the dimmer model, derived in Appendix A, only odd harmonics up to order 11 are considered. The turn on time, d, for the dimmer is chosen so that the dimmer is turned on two third of the time, that is, $d = T/6$ where T is the cycle time. The lamp resistance is $R_{lamp} = 600\,\Omega$. For comparison, a nonlinear time-domain model for an ideal dimmer is simulated to steady state. For the time domain modelling and simulation, the object oriented modelling language Omola and the simulation environment OmSim are used. Omola and OmSim are described in [Mattsson *et al.*, 1993],[Andersson, 1994].

In Figure 3.4, a voltage distortion of the third harmonic frequency is added to the fundamental frequency voltage. The plots show how the Fourier coefficients of the current are affected when a cosine or

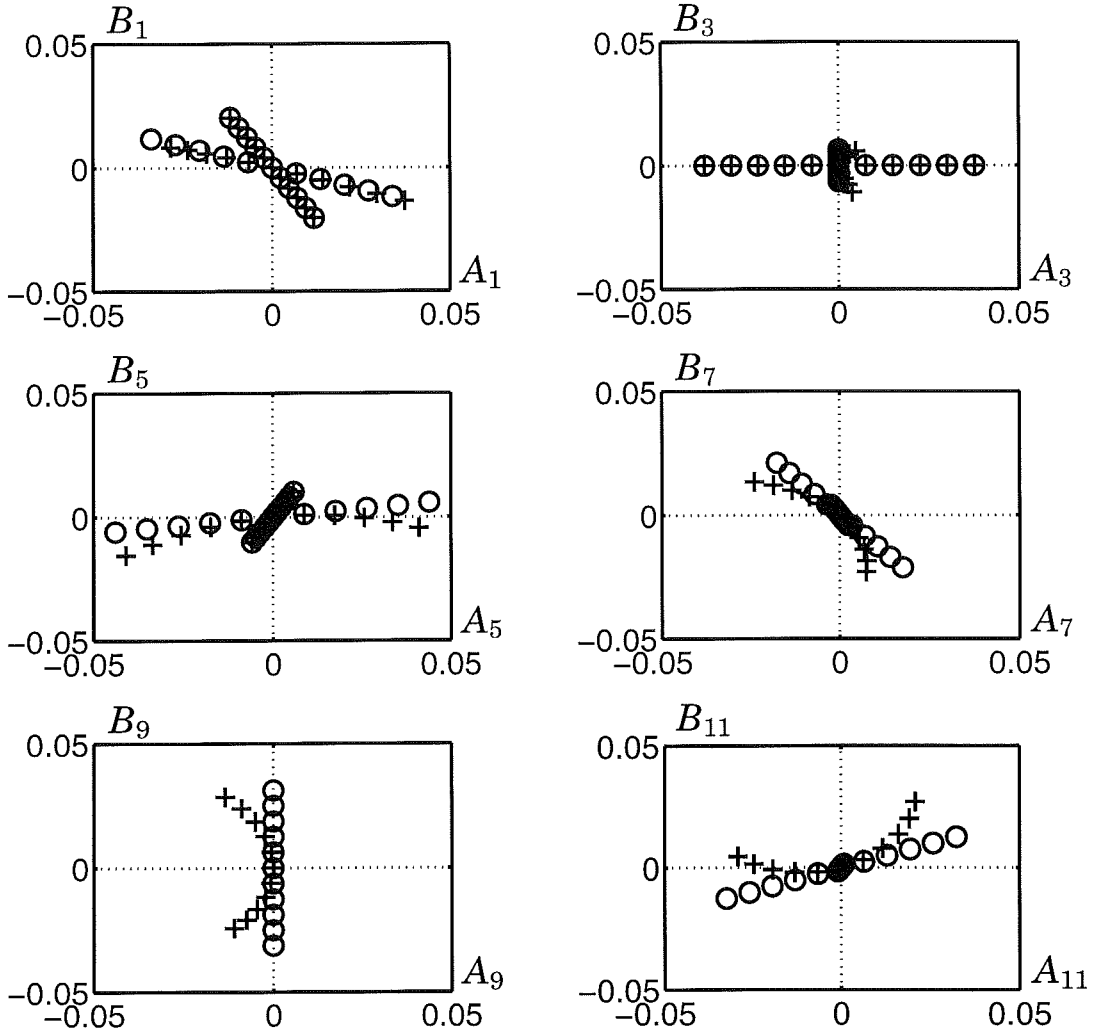

Figure 3.4 The plots show the deviation of the first six Fourier coefficient of the current through the dimmer, due to a third harmonic voltage disturbance. Each plot shows the result of a cosine disturbance and a sine disturbance. As the dimmer is linear with respect to a cosine disturbance, there is a perfect fit between the linear model (∘), and the nonlinear time domain model (+). For a sine disturbance, however, the result of the linearization is obvious. The larger the disturbance, the larger the misfit of the model.

sine disturbance is applied to the voltage, that is

$$v(t) = a_1^0 \cos \omega_0 t + \widehat{a}_3 \cos 3\omega_0 t, \text{ or}$$
$$v(t) = a_1^0 \cos \omega_0 t + \widehat{b}_3 \sin 3\omega_0 t.$$

For each frequency, the deviation in the sine coefficient of the current, B_k, is plotted against the deviation in the cosine coefficient, A_k. This

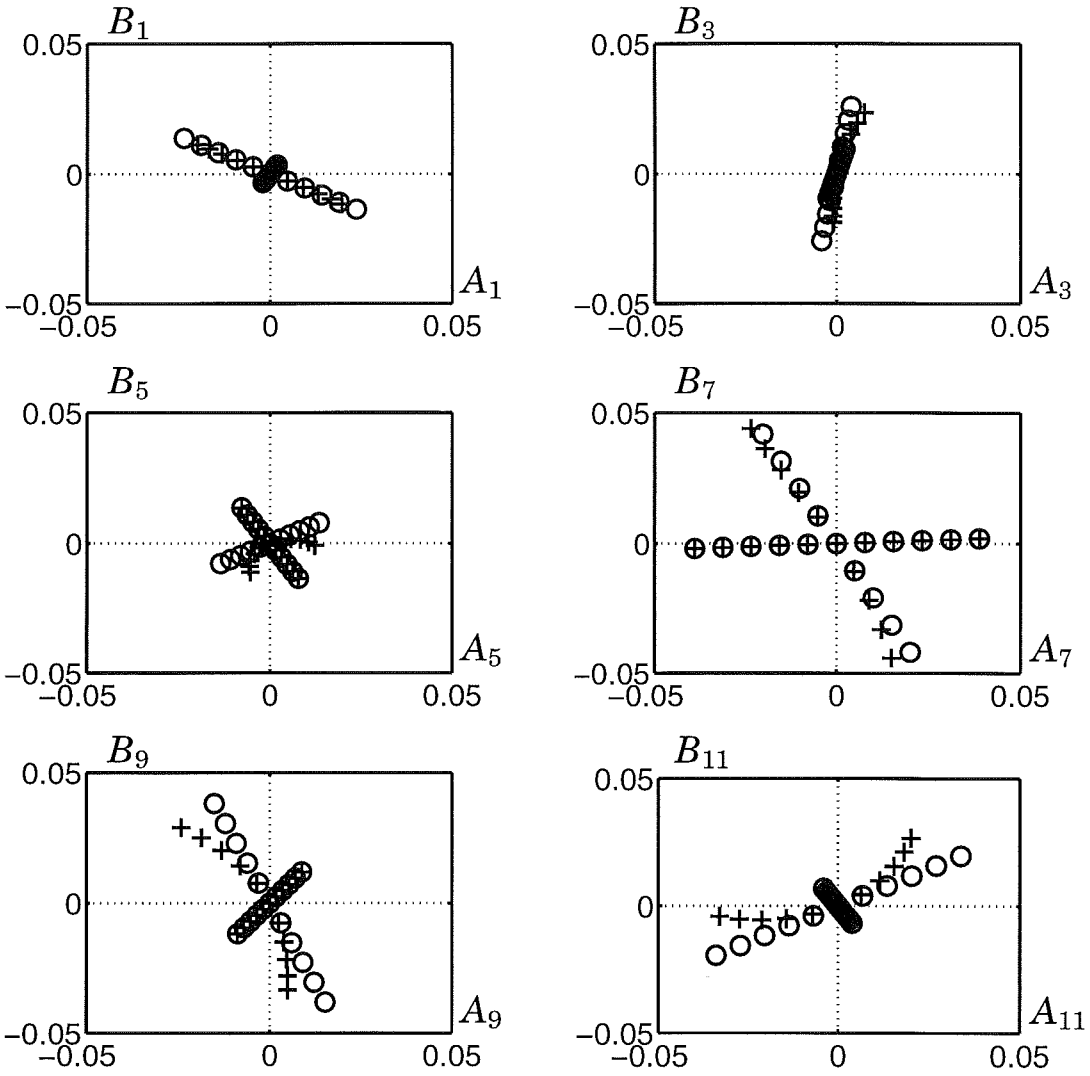

Figure 3.5 Plots showing the deviation from the nominal Fourier vector of the current at a seventh order voltage distortion. The result is similar to that of a third order distortion.

way, both phase and amplitude of the deviation is shown is one plot. The distortion amplitude, $\widehat{a}_3$ and $\widehat{b}_3$, range in steps of 2% from –10% to +10% of the nominal voltage, $a_1^0 = 230 \cdot \sqrt{2}\,\mathrm{V}$. The fundamental frequency is $\omega_0 = 2\pi \cdot 50\,\mathrm{rad/s}$.

For the linear model, that is, the Harmonic Norton Equivalents, the plots show equally spaced points on straight lines. A doubled voltage distortion amplitude results in a doubled amplitude for the current deviation, whereas the phase is the same. The calculations in Appendix A show that the dimmer is exactly linear with respect to a cosine distur-

bance. The reason for this is that a cosine disturbance does not affect the zero-crossing of the current, which determines the turn off time for the dimmer. This is shown in the plots, where there is a perfect fit for the linear model compared with a nonlinear model. For a sine disturbance, however, the result of the linearization is clearly seen. The larger the amplitude of the disturbance, the larger the deviations from the linear model.

Figure 3.5 shows the result of a voltage distortion of the seventh harmonic frequency. The accuracy of the Harmonic Norton Equivalent for this disturbance is similar to that of a third order disturbance.

A disturbance with an arbitrary phase can be seen as a superposition of a cosine disturbance and a sine disturbance. Thus for a dimmer, the worst case is a pure sine disturbance. It is shown that the linear model is a reasonably good approximation for amplitudes of the distortion limited to 6 % of the fundamental amplitude regardless of the phase of the disturbance.

Harmonic Norton Equivalents in Distribution Networks

The increasing use of power electronics has led to an increase in voltage distortion. This has given rise to a need for standards on allowed distortion levels, to guarantee a good power quality and also to determine how the responsibility for keeping the quality should be shared. In a proposal from STRI, see Appendix B, the maximum allowed distortion in Swedish distribution networks, is 4% for each harmonic component, and 6% total harmonic distortion (THD), for the voltage. These small allowed deviations from the nominal voltage justifies the linear relation, and indicates that the Harmonic Norton Equivalents are valid for analysis of networks under normal conditions.

3.3 Aggregation of Loads and Network Solving

The use of linearized models implies that aggregation of loads and network solving are non-iterative procedures using linear algebra. This results in fast solving without convergence problems. Furthermore, the Harmonic Norton Equivalents do not depend on the surrounding network. This means that aggregated models can be reused in other applications without being recalculated or measured.

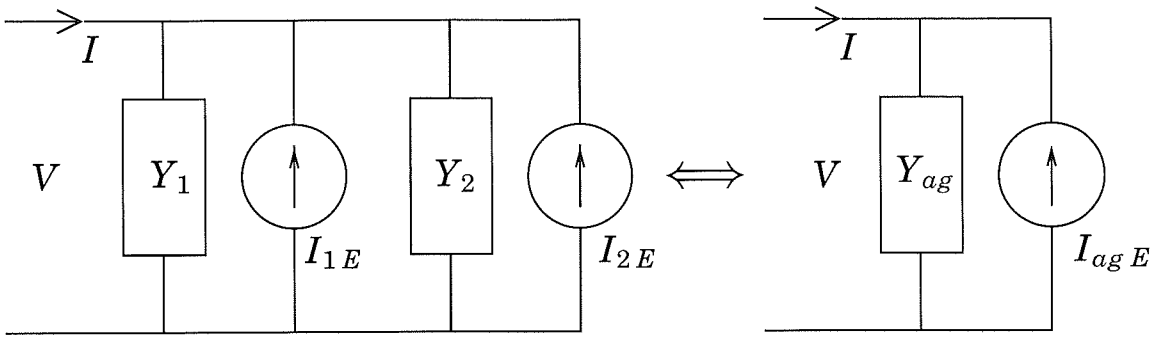

Figure 3.6 Two Harmonic Norton Equivalents in parallel are equivalently described by an aggregated model.

Aggregation of Two Parallel Loads

Aggregation of nonlinear loads is a straightforward procedure using Harmonic Norton Equivalents. As the voltage is the same across the two loads in parallel in Figure 3.6, the total current becomes

$$I = Y_1 V - I_{1E} + Y_2 V - I_{2E} = (Y_1 + Y_2)\, V - (I_{1E} + I_{2E})\,.$$

The aggregated model for the two Harmonic Norton Equivalents in parallel is thus achieved by simply adding the admittance matrices and the harmonic current sources respectively.

$$\begin{aligned} Y_{ag} &= Y_1 + Y_2, \\ I_{agE} &= I_{1E} + I_{2E}. \end{aligned} \tag{3.2}$$

Aggregation of Load and Net Impedance

Line losses affect the voltage across the components, and thus the current. It is possible to aggregate the line and the component. With the net impedance in series with the load, as in Figure 3.7, the voltage across the load is

$$V_1 = Y^{-1}\,(I + I_E)\,.$$

The current thus becomes

$$I = Y_{net}\,(V - V_1) = Y_{net}\left(V - Y^{-1}\,(I + I_E)\right).$$

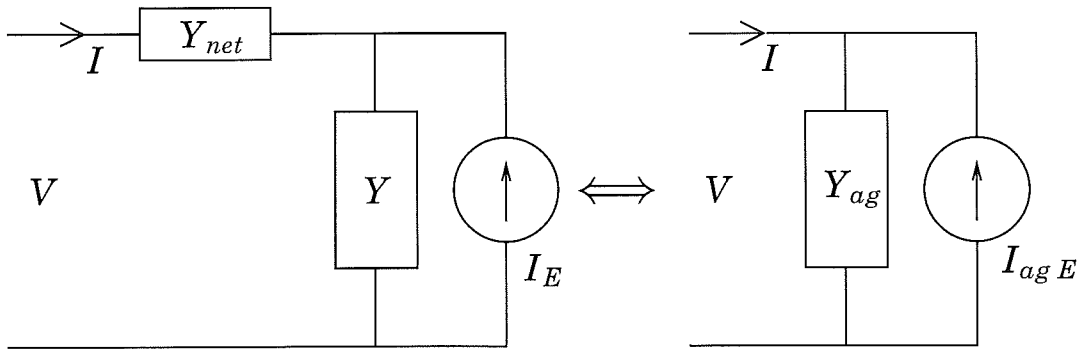

Figure 3.7 Line losses can be included in the Harmonic Norton Equivalent of a load.

Multiplying from the left with Y_{net}^{-1} and gathering all I-terms yields

$$\left(Y^{-1} + Y_{net}^{-1}\right) I = V - Y^{-1} I_E,$$

which gives for the current

$$\begin{aligned} I &= \left(Y^{-1} + Y_{net}^{-1}\right)^{-1} V - \left(Y^{-1} + Y_{net}^{-1}\right)^{-1} Y^{-1} I_E \\ &= \left(Y^{-1} + Y_{net}^{-1}\right)^{-1} V - \left(YY^{-1} + YY_{net}^{-1}\right)^{-1} I_E. \end{aligned}$$

The aggregated model for a nonlinear load connected in series with a line impedance is thus

$$\begin{aligned} Y_{ag} &= (Id + YY_{net}^{-1})^{-1} Y, \\ I_{ag\,E} &= (Id + YY_{net}^{-1})^{-1} I_E, \end{aligned} \tag{3.3}$$

where Id is the identity matrix, and Y_{net} is the admittance matrix for the net impedance. If the impedance is linear, Y_{net} is block diagonal, as stated in Chapter 2.

Solving a Small Network

The steady state solution of a network can be obtained by repetitive use of the rules for aggregation (3.2) and (3.3). This is used to calculate the total current, I_1, in the small network in Figure 3.8, with two dimmers in parallel, and small net impedances.

The two dimmers, with resistive loads of 20 Ω, are represented by Harmonic Norton Equivalents, $(Y_1,\ I_{1\,E})$ and $(Y_2,\ I_{2\,E})$. The reason for

chosing $R_{lamp} = 20\,\Omega$ instead of a $R_{lamp} = 600\,\Omega$ as in Section 3.2 is to get high enough currents, so that the voltage too gets distorted. The chosen R_{lamp} can be interpreted as 30 normal dimmed light bulbs at the same place in the network.

The net impedances, modelled as a resistor and an inductor in series, are represented by matrices, $Y_{net\,1}$ and $Y_{net\,2}$. The net resistances are $R_{net\,1} = 0.75\,\Omega$ and $R_{net\,2} = 0.25\,\Omega$, and the inductances are $L_{net\,1} = 0.0024\,H$ and $L_{net\,2} = 0.0008\,H$, respectively. The voltage source is purely sinusoidal, with RMS value 230 V and frequency 50 Hz.

The amount of distortion of the current through the dimmer is dependent on the turn on time, d, for the dimmer. If $d = 0$, the dimmer is on all the time, and it is thus linear and there is no current distortion. The longer the turn on time, the larger is the distortion. When $d = T/2$, where T is the cycle time, the dimmer is always off. To see if the accuracy depends on the level of distortion, the dimmer was simulated with the turn on time varying from zero to half a period. In Figure 3.9, the resulting current vector, I_1, is compared with the current obtained in a time domain simulation using OmSim. The plots show that the method works well for all d.

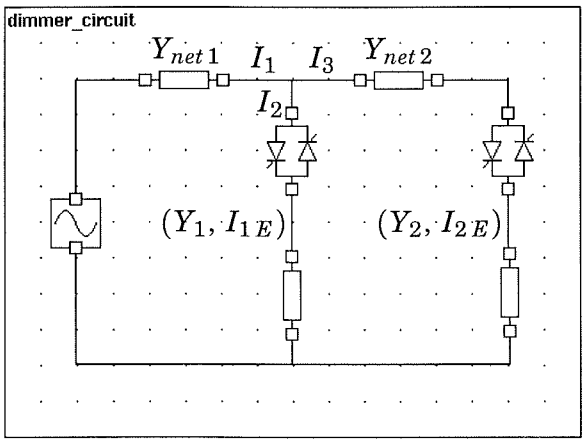

Figure 3.8 A small circuit with two dimmers, $(Y_1,\ I_{1E})$ and $(Y_2,\ I_{2E})$, and line losses, $Y_{net\,1}$ and $Y_{net\,2}$

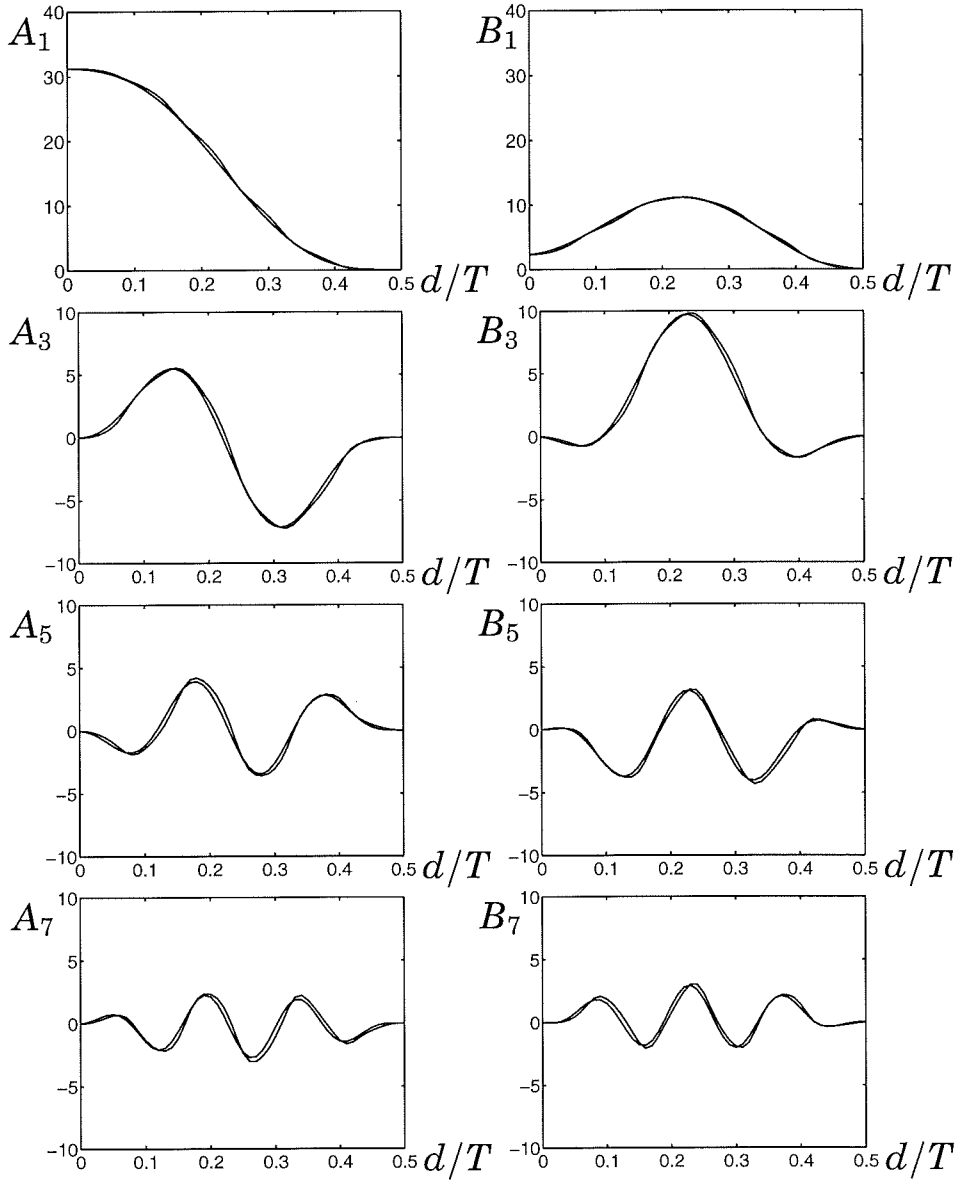

Figure 3.9 Plots showing the linearized and simulated Fourier coefficients for the current, I_1, in the circuit in Figure 3.8 as a function of the turn on time for the dimmers. When $d/T = 0.5$ the dimmer is permanently turned off.

3.4 Structure of the Admittance Matrix

For switching and dynamic components with memory, like the dimmer, there is no obvious structure in the Y-matrix. The matrix for a dimmer is shown in Appendix A.

If the nonlinear component is described by a static differentiable

relation, that is, if

$$i(t) = f(v(t)), \qquad \forall t,$$

where $f(v)$ is differentiable, then the Y-matrix can be shown to have a special structure. Recall

$$\begin{aligned} i(t) &= \sum_{k=1}^{N} A_k \cos k\omega_0 t + B_k \sin k\omega_0 t = f\left(v(t)\right), \\ v(t) &= \sum_{k=1}^{N} a_k \cos k\omega_0 t + b_k \sin k\omega_0 t, \end{aligned}$$

The Fourier coefficients of the current, A_k and B_k, are defined as

$$\begin{aligned} A_k &= \frac{2}{T}\int_t^{t+T} f(v(t)) \cos k\omega_0 t \, dt, \\ B_k &= \frac{2}{T}\int_t^{t+T} f(v(t)) \sin k\omega_0 t \, dt, \end{aligned}$$

where $T = \frac{2\pi}{\omega_0}$ is the cycle time. The partial derivatives of the cosine coefficients are

$$\begin{aligned} \frac{\partial A_k}{\partial a_l} &= \frac{2}{T}\int_t^{t+T} \frac{df}{dv}\frac{\partial v}{\partial a_l} \cos k\omega_0 t \, dt \\ &= \frac{2}{T}\int_t^{t+T} \frac{df}{dv} \cos l\omega_0 t \cos k\omega_0 t \, dt \\ &= \frac{1}{T}\int_t^{t+T} \frac{df}{dv} (\cos(k+l)\omega_0 t + \cos(k-l)\omega_0 t) \, dt \\ &= h_{11}(k+l) + t_{11}(k-l). \end{aligned}$$

The other elements of the Y-matrix are obtained similarly

$$\begin{aligned}
\frac{\partial A_k}{\partial b_l} &= \frac{2}{T}\int_t^{t+T} \frac{df}{dv} \sin l\omega_0 t \cos k\omega_0 t \, dt \\
&= \frac{1}{T}\int_t^{t+T} \frac{df}{dv} (\sin(k+l)\omega_0 t - \sin(k-l)\omega_0 t) \, dt \\
&= h_{12}(k+l) + t_{12}(k-l), \\
\frac{\partial B_k}{\partial a_l} &= \frac{2}{T}\int_t^{t+T} \frac{df}{dv} \cos l\omega_0 t \sin k\omega_0 t \, dt \\
&= \frac{1}{T}\int_t^{t+T} \frac{df}{dv} (\sin(k+l)\omega_0 t + \sin(k-l)\omega_0 t) \, dt \\
&= h_{21}(k+l) + t_{21}(k-l), \\
\frac{\partial B_k}{\partial b_l} &= \frac{2}{T}\int_t^{t+T} \frac{df}{dv} \sin l\omega_0 t \sin k\omega_0 t \, dt \\
&= \frac{1}{T}\int_t^{t+T} \frac{df}{dv} (-\cos(k+l)\omega_0 t + \cos(k-l)\omega_0 t) \, dt \\
&= h_{22}(k+l) + t_{22}(k-l).
\end{aligned}$$

The derivatives are functions of $k+l$ and $k-l$. The Y-matrix can thus be written as the sum of a block Hankel matrix, H, and a block Toeplitz matrix, T,

$$Y = \frac{dI}{dV} = H + T,$$

where

$$H = \begin{bmatrix} h_2 & h_3 & h_4 & \dots & h_{N+1} \\ h_3 & h_4 & h_5 & \dots & h_{N+2} \\ h_4 & h_5 & h_6 & \dots & h_{N+3} \\ \vdots & \vdots & \vdots & \ddots & \vdots \\ h_{N+1} & h_{N+2} & h_{N+3} & \dots & h_{2N} \end{bmatrix}, \qquad h_i = \begin{bmatrix} h_{11}(i) & h_{12}(i) \\ h_{21}(i) & h_{22}(i) \end{bmatrix},$$

$$T = \begin{bmatrix} t_0 & t_{-1} & t_{-2} & \dots & t_{-N+1} \\ t_1 & t_0 & t_{-1} & \dots & t_{-N+2} \\ t_2 & t_1 & t_0 & \dots & t_{-N+3} \\ \vdots & \vdots & \vdots & \ddots & \vdots \\ t_{N-1} & t_{N-2} & t_{N-3} & \dots & t_0 \end{bmatrix}, \qquad t_i = \begin{bmatrix} t_{11}(i) & t_{12}(i) \\ t_{21}(i) & t_{22}(i) \end{bmatrix}.$$

This structure reduces the number of measurements required when estimating the models experimentally in Chapter 4.

3.5 Summary

The Harmonic Norton Equivalent has been presented as a compact way of describing the harmonic behaviour of aggregated loads in distribution networks. The linearization has been validated for a dimmer for acceptable distortion levels in distribution networks under normal operation. Aggregation of loads has been shown to be a straightforward non-iterative procedure. How aggregated loads can be obtained through real measurements, thus avoiding involved detailed load modelling, is shown in Chapter 4.

4

Harmonic Norton Equivalents from Measurements

An important feature of the Harmonic Norton Equivalents is that they can be obtained from measurements. Detailed, complicated frequency domain modelling is avoided by obtaining aggregated models experimentally. A procedure for numerical estimation of Harmonic Norton Equivalents through measurements or time domain simulation is presented in this chapter.

4.1 An Estimation Procedure

A procedure for obtaining the models from sampled time domain signals is proposed in four steps:

1. Determine the nominal current, $i_0(t)$, by applying the nominal voltage, $v(t) = a_0 \cos \omega_0 t$, where a_0 is the nominal amplitude, and ω_0 is the fundamental frequency.

2. Measure current and voltage for, at least, $2N$ different small periodic distortions from the nominal wave shape of the voltage.

For example

$$\begin{aligned} v(t) &= a_0 \cos \omega_0 t + \widehat{a}_k \cos k\omega_0 t \\ v(t) &= a_0 \cos \omega_0 t + \widehat{b}_k \sin k\omega_0 t \end{aligned} \qquad k = 1, 2, \ldots, N. \tag{4.1}$$

3. Use the Discrete Fourier Transform to calculate current and voltage spectra from the sampled time domain signals. The nominal spectra are called I_0, and V_0, respectively, and let I_k, and V_k represent the spectra from the kth distorted measurement.
4. The admittance matrix Y is obtained through the linear equation system

$$Y\widehat{V} = \widehat{I}, \tag{4.2}$$

where

$$\begin{aligned} \widehat{V} &= [\, V_1 - V_0 \quad V_2 - V_0 \quad \ldots \quad V_{2N} - V_0 \,], \\ \widehat{I} &= [\, I_1 - I_0 \quad I_2 - I_0 \quad \ldots \quad I_{2N} - I_0 \,]. \end{aligned}$$

Finally, the harmonic current source, I_E, is derived

$$I_E = YV_0 - I_0.$$

4.2 Some Comments on the Procedure

Step 1

The current through a nonlinear component contains harmonics, and if the voltage source is not stiff, the voltage across the component will also contain harmonics. This means that the behaviour of the component for small distortions around the nominal voltage is not measured, but the behavior around a distorted voltage, $\widetilde{v}_0$. This is the same as linearizing around another linearization point. If v_0 and $\widetilde{v}_0$ are close, the linearization is still valid, and the Y-matrix can be used to derive the nominal current spectrum

$$I_0 = \widetilde{I}_0 + Y(V_0 - \widetilde{V}_0).$$

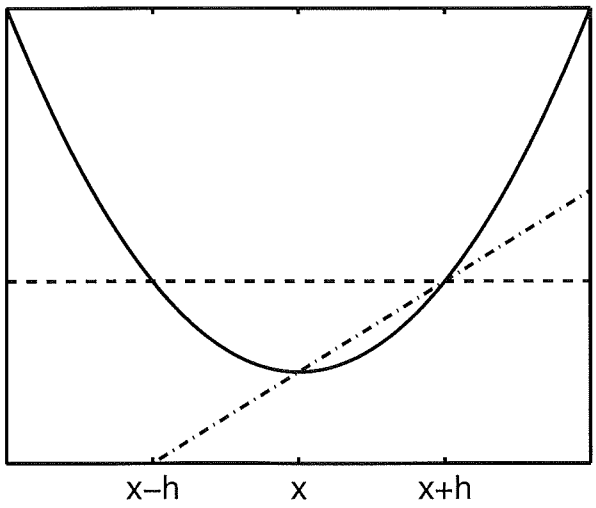

Figure 4.1 Estimating the derivative using the forward difference (dash-dotted) and the central difference (dashed).

Steps 2 & 4

To get good numerical accuracy, the matrix $\widehat{V}$ in Equation 4.2 needs to be well conditioned. This is obtained by distorting only one of the Fourier coefficients of the voltage for each measurement, aiming for a diagonal $\widehat{V}$.

Just like in Step 1, with a weak voltage source, the distorted voltage will not contain only the two frequencies, ω_0 and $k\omega_0$. In order to get $\widehat{V}$ well conditioned, these two frequencies should dominate. This, together with measurement noise, sets a lower limit on the amplitudes $\widehat{a}_k$ and $\widehat{b}_k$ in Equation (4.1).

The elements in Y are derivatives of the current Fourier coefficients and describe the local behaviour in the neighbourhood of the nominal voltage. Increased voltage deviations imply poorer estimates of these derivatives and, thus, poorer estimates of the elements in Y.

Better estimates of the derivatives are obtained if the central difference is used

$$\frac{d}{dt}f(x) = \frac{f(x+h) - f(x-h)}{2h} + O(h^2),$$

instead of the forward difference

$$\frac{d}{dt}f(x) = \frac{f(x+h) - f(x)}{h} + O(h).$$

However, this requires twice as many measurements. For the voltages in Equation (4.1), both positive and negative values of the distortion amplitudes, $\widehat{a}_k$ and $\widehat{b}_k$, are required. Using the central difference, $\widehat{V}$ and $\widehat{I}$ in (4.2) becomes

$$\widehat{V} = [\, V_1 - V_{-1} \quad V_2 - V_{-2} \quad \dots \quad V_{2N} - V_{-2N} \,],$$
$$\widehat{I} = [\, I_1 - I_{-1} \quad I_2 - I_{-2} \quad \dots \quad I_{2N} - I_{-2N} \,].$$

The advantage of using the central difference is shown in Figure 4.1. Even with a large h the derivative is well approximated, at least if the nonlinear functions are approximately quadratic, like for the dimmer in Section 3.2.

Another problem with a non-stiff voltage source is that all frequencies that are apparent in the voltage must be considered in the estimation experiment. This means that even though the configuration of the network implies that, for instance, there cannot be a fifth harmonic component in the signals, this frequency has to be considered in the model during the estimation procedure. The model can be reduced afterwards, to exclude the fifth harmonic, by means of model reduction techniques. However, when estimating parameters it is necessary to have a model that includes all frequencies that appear in the measurements. Unfortunately, more measurements are then needed as there are more parameters to estimate.

A more straightforward way would be to use the natural variations in harmonic voltage distortion, to obtain the N measurements. This does not guarantee that the $\widehat{V}$-matrix becomes well conditioned, but the model will probably be accurate the kind of disturbances that are common, and thus used in the estimation.

Step 3

The Discrete Fourier Transform (DFT) facilitates a way to obtain the Fourier coefficients of a signal from finite time sampled data. The DFT,

$X(k)$, of a sampled signal, $x(n)$, is defined as

$$\begin{aligned} X(k+1) &= \sum_{n=0}^{N-1} x(n+1)e^{-j\frac{2\pi kn}{N}}, \\ x(n+1) &= \frac{1}{N}\sum_{k=0}^{N-1} X(k+1)e^{j\frac{2\pi kn}{N}}. \end{aligned} \tag{4.3}$$

A popular and efficient implementation of the DFT is the Fast Fourier Transform (FFT) [Oppenheim and Schafer, 1989]. The FFT is used by tools like Matlab.

The DFT assumes a periodic extension of the finite data series. If the signal contains frequencies that are not within the basis set $\left\{e^{j\frac{2\pi kn}{N}}\right\}$ of the DFT, the periodic extension becomes discontinuous. The discontinuities affect all Fourier coefficients $X(k)$. This is called spectral leakage. To avoid spectral leakage, the sampled data series is multiplied with a window function that makes the periodic extension of the signal and its derivatives continuous.

The choice of window for the Fourier transform depends on several factors, for instance noise and disturbances, and also how close to perfect periodicity the signals are [Harris, 1978]. The importance of windows to avoid spectral leakage when measuring Harmonic Norton Equivalents is obvious, as the fundamental frequency is very dominant. The amplitudes of the harmonic frequencies are normally just a few percent of the fundamental frequency amplitude. Thus, the spectral leakage between harmonic frequencies must be much less than one percent. As multiplication of a window in the time domain is equivalent to a convolution with the Fourier transform of the window in the frequency domain, this means that the amplitude of the Fourier transform of the window must be small for frequencies $\omega = \pm m\omega_0$, where m is an integer.

4.3 Comparison with Estimation of Linear Loads

For linear systems, a single frequency input results at steady state in an output of the same frequency. Different frequencies can be treated

separately, and the resulting output is a superposition of all frequencies in the input. For nonlinear systems, this is not the case. A sinusoidal input will at steady state give an output with not only the same frequency, but harmonic frequencies, and possibly sub-harmonic frequencies, too. When linearizing the system around the nominal voltage, it is measured how a small voltage superimposed to the nominal one affects the nominal current spectrum. A small voltage distortion of a harmonic frequency affects all current harmonics and not just the current component with the same frequency as the added voltage. Furthermore, the current variations depend on both frequency and phase of the superimposed voltage.

When sampling a continuous time signal, an anti-aliasing filter must be used to avoid aliasing problems. The sensors used for the measurements may also be low pass filtering. The filters affect the amplitude and the phase of the signals. When estimating linear systems, this does not cause any problems, because both inputs and outputs are affected in the same way, as the different frequencies are considered separately. With nonlinear loads, however, the signals contain many frequencies at the same time. As the filter effects are different for different frequencies, the dynamics of the filter must be known and compensated for.

4.4 An Example: The Dimmer

In this section, the procedure described in Section 4.1 is used to measure the model parameters for a light dimmer. The model is validated by applying a perturbed voltage to the dimmer, and comparing the current predicted by the model with the measured current. The predicted current matches the validation data almost perfectly. The result shows that the method has a great potential.

The Process

The dimmer was briefly described in Section 3.2, and in Appendix A, there is a more detailed description of how it works. A dimmer is a simple but highly non-linear component and serves as a good test component to validate our method.

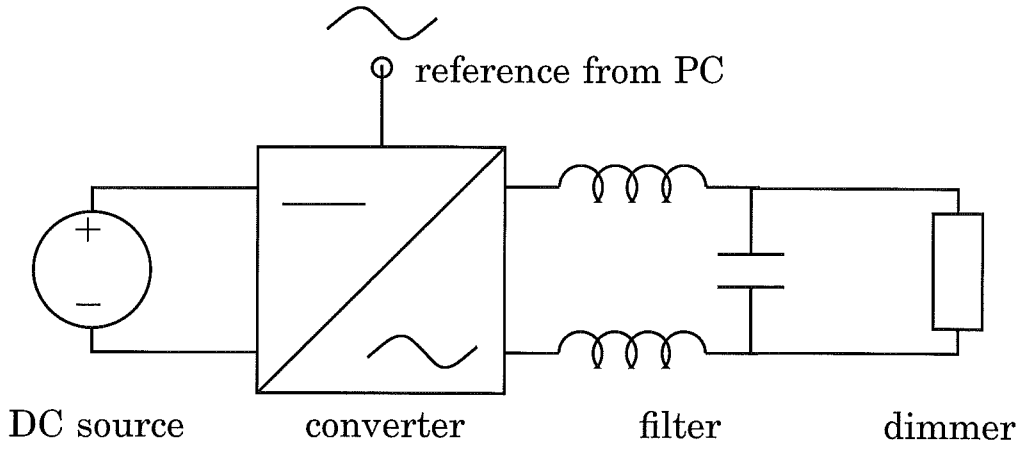

Figure 4.2 A schematic of the experiment setup.

Shaping the voltage

The experiment setup is shown in Figure 4.2. A switched voltage converter is used to produce a PWM waveform. The pulse width is proportional to a reference signal, which is calculated and output from a PC. The converter switching frequency is 4 kHz. To get rid of the high frequencies generated by the switching, a low pass LCL-filter with a bandwidth of 3 kHz is used to smooth the voltage.

Measurement Equipment

The Daqbook Data Acquisition System from IO-tech, [IOtech, 1995], is used to measure voltage and current. The current is measured with a current probe (LEM HEME PR 30). It is filtered through an analog anti-aliasing filter (DBK 18 Filter Module from IOtech, with a bandwidth of 1 kHz). To avoid damage of the equipment, the voltage is measured with a high voltage insulation unit in the Daqbook. This voltage insulation unit low pass filters the voltage, with approximately the same bandwidth as the current ($\approx$ 1 kHz). The frequency responses of the two filters, obtained using a Solatron frequency analyzer, are shown in Figures 4.3 and 4.4, and the results are used to compensate for the filters in the estimation experiments for the dimmer model.

The Daqbook samples at a maximum frequency of 100 kHz and measures up to 256 analog signals. For the experiments, a sampling rate of 23.810 kHz is used, and the duration of each measurement is 1 s. The reason for the fast sampling rate is that the documentation of

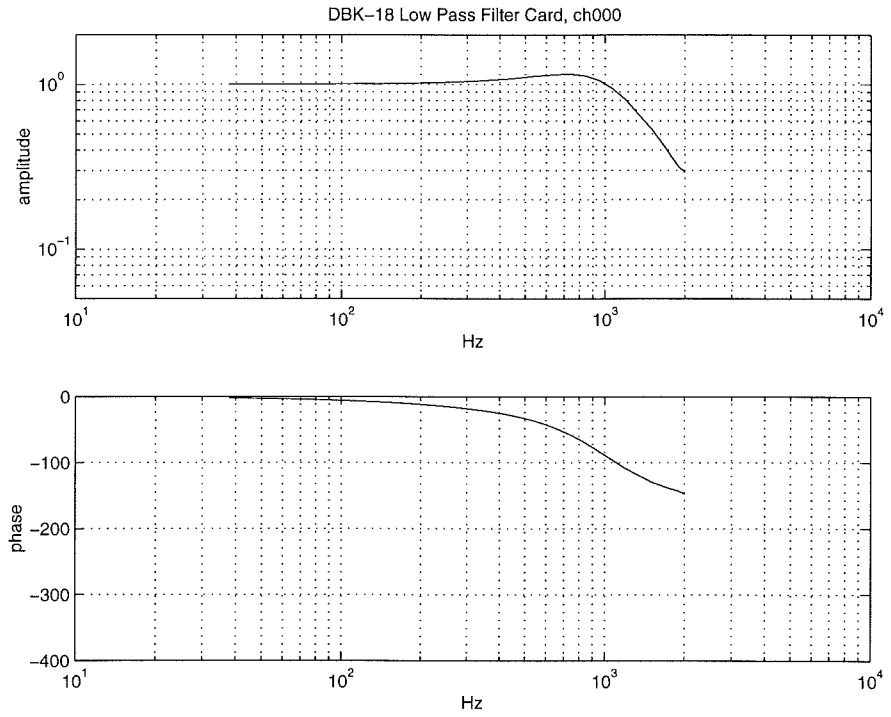

Figure 4.3 The Bode plots of the anti-aliasing filter used to filter the current signal. The bandwidth is 1 kHz.

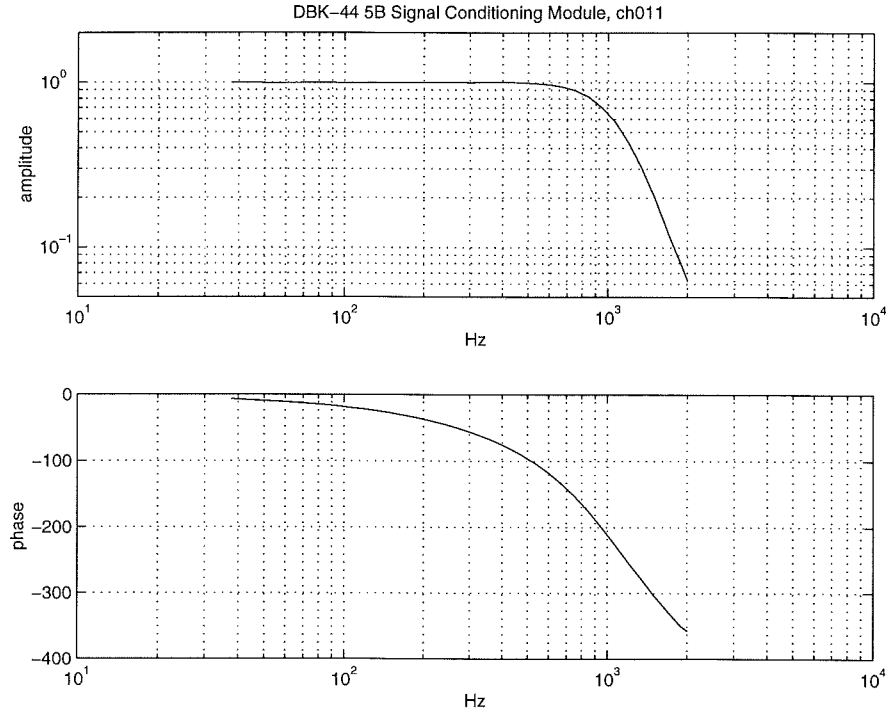

Figure 4.4 The Bode plots of the voltage insulation unit. The bandwidth is approximately 1 kHz.

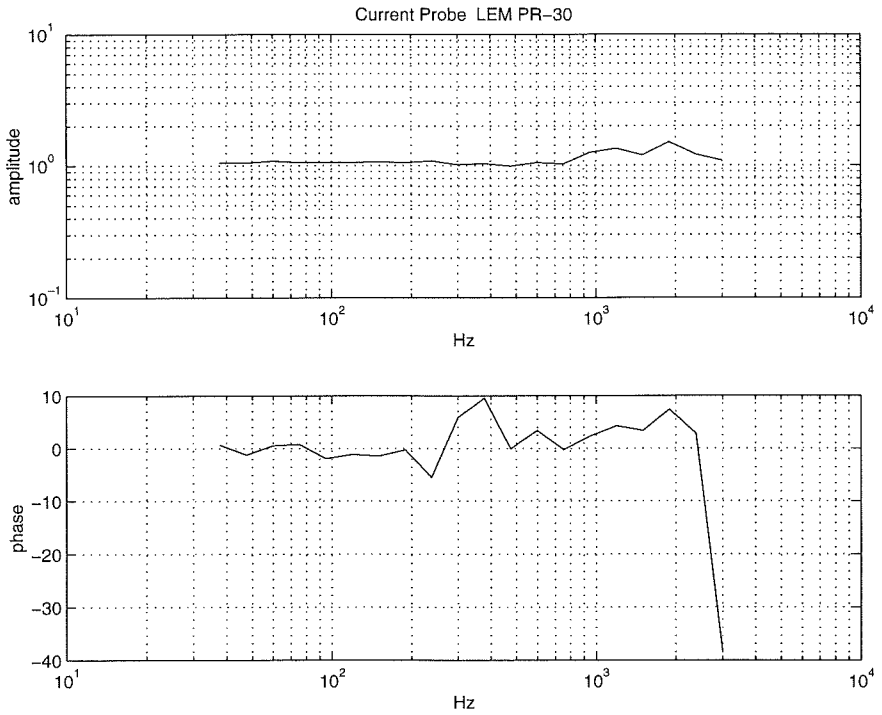

Figure 4.5 The Bode plot for the current probe. The bandwidth of the probe is much higher than the frequencies considered in the model.

the Daqbook does not say that the voltage insulation unit is low pass filtering. To avoid aliasing of the voltage, the sampling frequency is chosen as fast as possible without being a multiple of the fundamental frequency of the voltage. The latter avoids high frequency harmonics to be folded down exactly at lower frequency harmonics. As mentioned before, a frequency analysis of the insulation unit showed that it indeed low pass filters the voltage, which means that the sampling rate is unnecessarily high.

The Bode plot for the current probe was also obtained using the Solatron frequency analyzer, see Figure 4.5. The plot shows that the bandwidth of the probe is much higher than the frequencies we considered, and the dynamics of the probe is therefore neglected in our experiments. The phase is not constant, probably due to resonances. However, the maximum phase shift is less that 10 degrees.

4.5 The Estimation Procedure

Step 1

The use of the DC generator and the low pass filter results in a weak voltage source. The current and the voltage, when the voltage reference is a clean 50 Hz sinusoid, is shown in Figure 4.6. The plots show that there is a considerable amount of distortion also in the voltage. However, the measurement data show a very good periodicity, and a very low noise level. According to the comments in Section 4.2, this means that the voltage source can still be used.

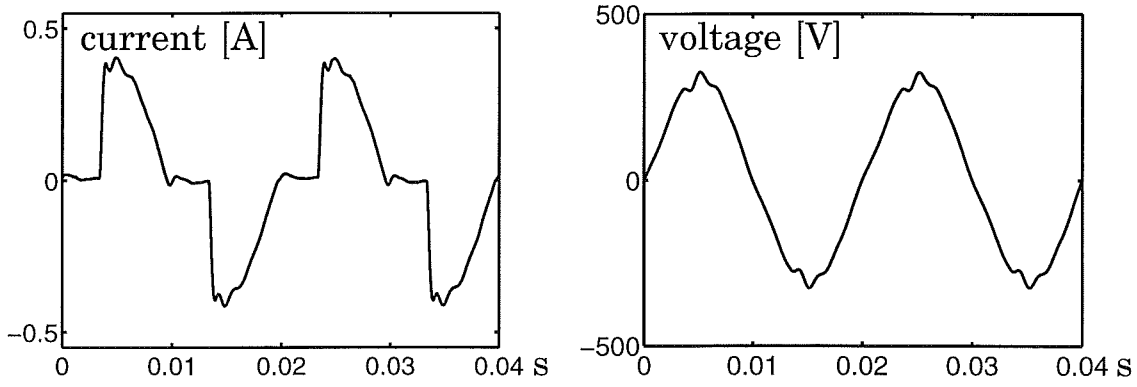

Figure 4.6 Measured current and voltage from a light dimmer.

Step 2

As the dimmer is approximately symmetric, like most electric loads, only odd harmonics are considered. Figure 4.7 shows that the voltage contains a fair amount of odd harmonics up to order 13. Therefore, the estimated model includes these frequencies. To get $\widehat{V}$ well conditioned, the amplitudes of the added voltage distortions, $\widehat{a}_k$ and $\widehat{b}_k$, are set to be 5% of the nominal voltage. The condition number of the matrix is 6.8, which must be considered acceptable.

A close look at the current plot in Figure 4.6 shows that the dimmer is not exactly symmetric. When the dimmer is turned off, and the current is approximately zero, the shape of the curve is not exactly the same for positive and negative voltage. This results in harmonics of even order, which, however, are being considered in the model. There

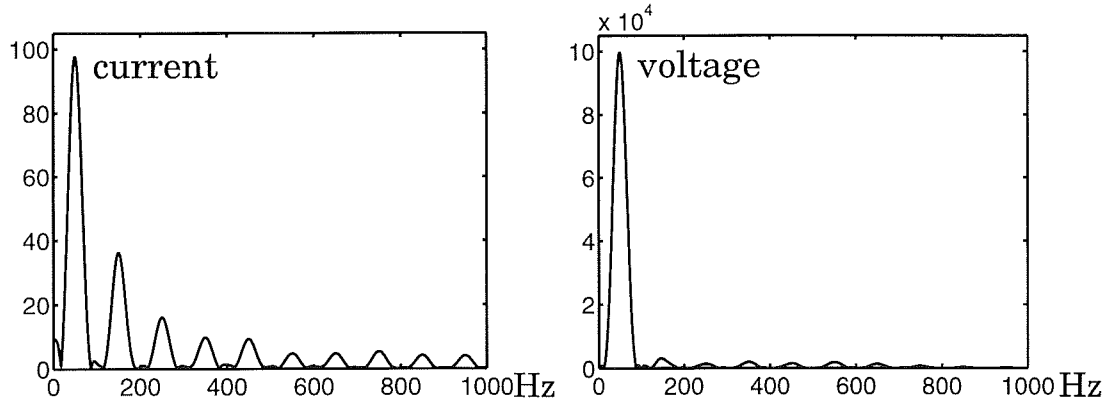

Figure 4.7 The current and voltage spectra from measurements on the dimmer. The spectra are obtained using a Kaiser window.

are also low amplitude harmonics of order higher than 13.

Step 3

Matlab's Signal Processing Toolbox [Mathworks, 1996] is used to analyze the sampled signals. The signals shows a very low noise level, and a good periodicity. The only criteria for the choice of window, is thus that the spectral leakage between harmonic frequencies shall be minimized, and the peaks detected accurately. In the analysis below, a Kaiser window with $L = 1263$, and $\beta = 5.48$, is used. It is chosen so that the Fourier transform of the window has dips for $f = \pm 50\,\text{Hz}$, and $f = \pm 100\,\text{Hz}$, to minimize spectral leakage, see Figure 4.8.

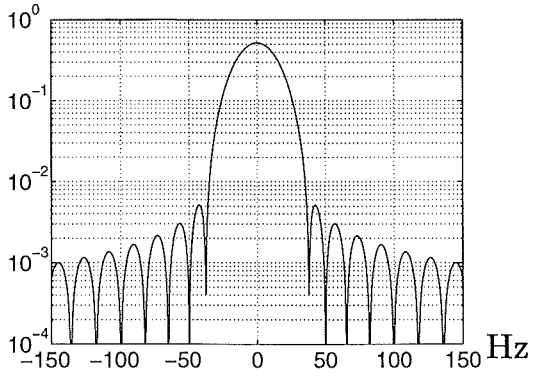

Figure 4.8 Fourier transforms of a Kaiser window with $L = 1263$ and $\beta = 5.48$. The window has been chosen to have minimal spectral leakage for periodic signals with frequency 50 Hz.

4.6 Validation of the Dimmer Model

In order to check whether the procedure gives accurate models, the estimated dimmer model is validated by comparing predicted current spectra with measured spectra for three different voltage distortions.

The validation series Data 1 and Data 2 consist of measured voltages and currents from the experiment setup. Data 3 has the line voltage from a wall socket as source. All series show a level of distortion that is higher than what is allowed in distribution networks. The voltage distortions from the three measurement series are shown in Figures 4.9 and 4.10.

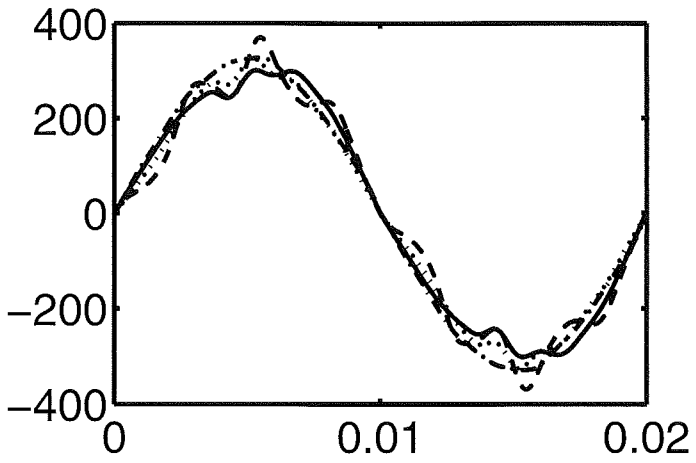

Figure 4.9 The different voltage distortion used to validate the estimated model. The nominal voltage is dotted, Data 1 is solid, Data 2 is dashed, and Data 3 is dash-dotted.

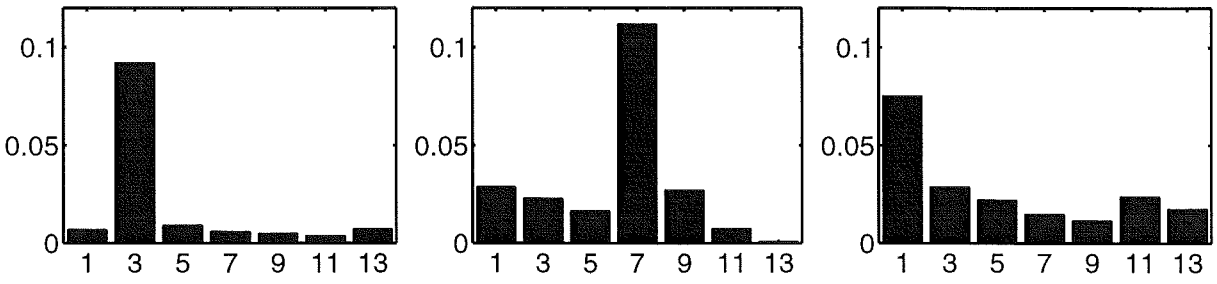

Figure 4.10 Amplitude spectra for the voltage distortions used to validate the estimated model. The amplitudes are normalized with respect to the nominal voltage amplitude.

Data 1

Data 1 has most of its distortion in the third harmonic and a total harmonic distortion (THD) of 9%. The result from the validation of the model is shown in Figure 4.11. The upper plot shows the deviation from the nominal current, shown in Figure 4.6. The estimated deviation is solid, whereas the measured one is dashed. The lower plots show amplitude and phase of the deviation from the nominal current spectrum. The left plot shows the amplitude of the deviation in per-

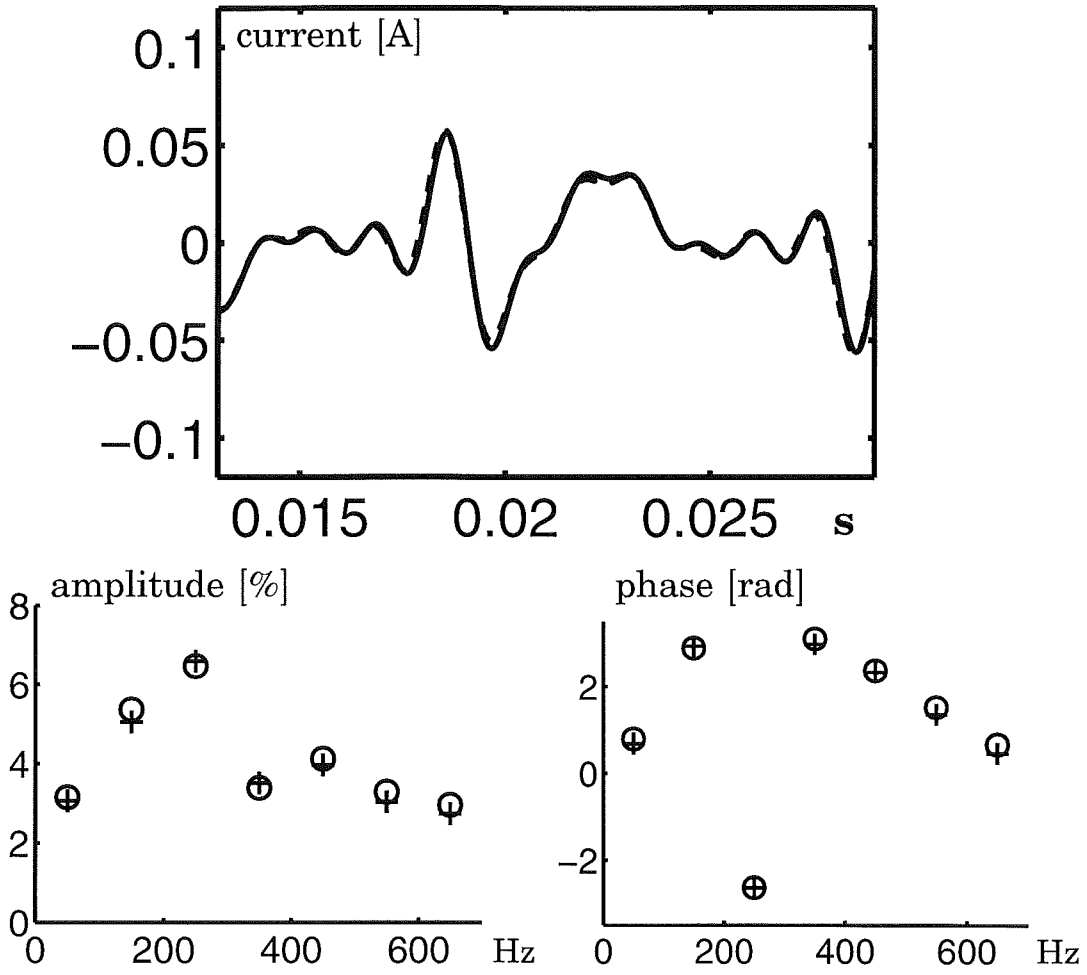

Figure 4.11 Validation of the model using Data 1. The upper plot shows the deviation from the current due to the voltage distortion. The estimated current is solid, whereas the measured current is dashed. The lower plots show amplitude and phase of the Fourier coefficients of the current. Estimated values are marked with rings, (o), and measured values with a plus, (+). There is an almost perfect match between estimated and measured current.

cent of the nominal fundamental frequency component. The right plot shows the phase of the deviation in rad/s. The values estimated with the models are marked with a ring, (o), and the real measured values are marked with a plus, (+). For Data 1, there is an almost perfect match between the estimated and measured current.

Data 2

Data 2 has most of its distortion in the seventh harmonic and the THD is 12%. Figure 4.12 shows a little larger deviations than for Data 1, but still the result is very good. The phase is still very good, but there are small errors in amplitude. One explanation for the mismatch can be that the forward difference was used for estimating the derivatives

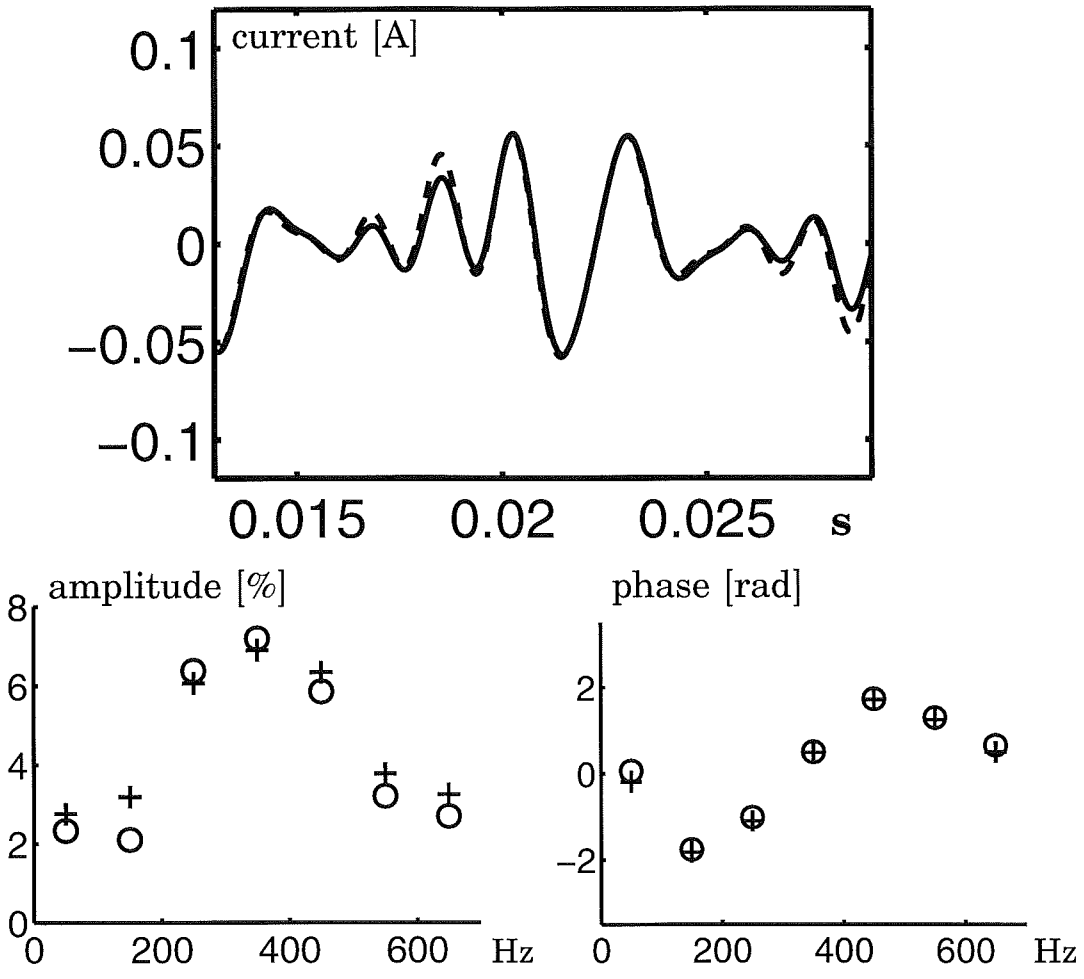

Figure 4.12 Validation of the model using Data 2.

in the model, and that the dominating voltage distortion (7th order) has negative amplitude. The central difference would almost certainly give a better result for Data 2, as discussed in Section 4.2. However, considering the high level of distortion, the result is still very good.

Data 3

The voltage in Data 3 is almost distortion free, but compared to the nominal voltage used in the estimation procedure, there is a considerable amount of distortion in all harmonic frequencies, and a THD of 9%. What is interesting with this data series is that there are large deviations also for harmonic frequencies of order higher than 13. A good result justifies the use of truncated Fourier series. The result from the

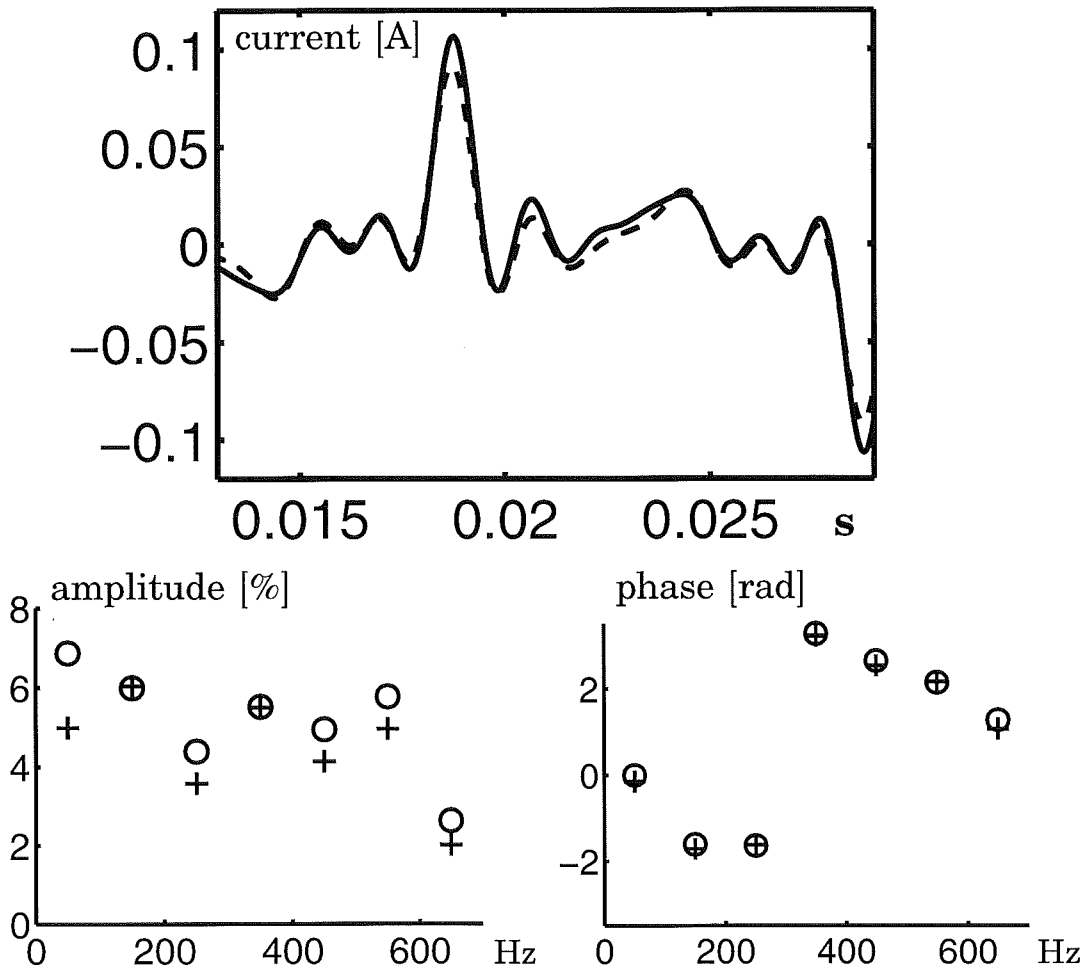

Figure 4.13 Validation of the model using Data 3.

validation using Data 3 is shown in Figure 4.13. The plots show that the result is very good, even though the distortion level is high.

4.7 Discussion

A procedure for estimation of Harmonic Norton Equivalents has been presented. The procedure uses sampled data from measurements or from time domain simulations. A model for a simple light dimmer is obtained from real measurements to describe the procedure. The validations show that the resulting Harmonic Norton Equivalent is a very good description of the dimmer even at high voltage distortion levels.

The experiments were made in a lab environment, with little noise and almost periodic signals. In real applications, the results are probably dependent on proper signal processing. To decrease the variance, the sampled signals are split into smaller segments. The length of each segment is equal to the length of the window. Each segment is Fourier transformed, and the mean value of all segments is chosen as the final result. The more segments there are, the smaller is the variation. This means that it is desired to have as short windows as possible. Short windows, however, result in wide main lobes and thus poor resolution. The final choice of window must be a compromise.

The worst source of error is probably the voltage source used in the estimation process. The power electronic devices used to convert direct voltage to the desired shape are very temperature dependent. The voltage source is also weak, which results in a considerable degree of distortion even for high order harmonics. With a more suitable voltage source, the result would most certainly be even better.

5

Conclusions and Future Work

Many power electronic devices can, if properly controlled, be used to improved the quality of the supplied power. A novel approach to modelling of electric loads has been presented in this thesis. The aim has been to obtain simple, low order models, suitable for stability and robustness analysis and control design.

The proposed Harmonic Norton Equivalent is a linearized description of the relation between current and voltage in frequency domain. The linearization implies that aggregation of loads and network solving is performed using linear algebra. Common iterative frequency domain methods are avoided, and thus any convergence problems associated with the iteration. Rules for aggregation of loads have been derived, and the aggregated models show a good accuracy.

A procedure for experimental estimation of models has been presented. It can be used either for real measurements or for obtaining models using time domain simulation. The procedure reveals a number of difficulties with estimation of nonlinear models.

The light dimmer has been used as an example throughout the thesis. The Harmonic Norton Equivalent for a dimmer with ideal switching was derived and used to show that the accuracy of the model structure is satisfying under voltage distortions within the allowed limits. The model for a real dimmer was estimated using the proposed procedure. The obtained model shows a good agreement with the validation data.

Future Work

Future work includes the following:

- *error analysis:* How are the errors introduced by the linearization and the truncation affected by the aggregation of loads?
- *stability analysis:* How can ideas from stability analysis of linear systems be used to analyze the proposed models?
- *resonances:* How are resonance problems detected and solved?
- *filter design:* How should filters for harmonic mitigation be designed?
- *transient analysis:* The model structure is derived for steady state analysis. Is it possible to use it for transient analysis too?
- *improved experiments:* Are there more simple ways to obtain the models from measurements?

6

Bibliography

ACHA, E., J. ARRILLAGA, A. MEDINA, and A. SEMLYEN (1989): "General frame of reference for analysis of harmonic distortion in systems with multiple transformer nonlinearities." *IEE Procedings*, **136C:5**, pp. 271–278.

ANDERSSON, M. (1994): *Object-Oriented Modeling and Simulation of Hybrid Systems*. PhD thesis ISRN LUTFD2/TFRT--1043--SE, Department of Automatic Control, Lund Institute of Technology, Box 118, S-22100 Lund, Sweden.

ARRILLAGA, J. and C. D. CALLAGHAN (1991): "Three phase AC-DC load and harmonic flows." *IEEE Trans. on Power Delivery*, **6:1**, pp. 238–244.

ARRILLAGA, J., A. MEDINA, M. L. V. LISBOA, M. A. CAVIA, and P. SÁNCHEZ (1994): "The harmonic domain. A frame of reference for power system harmonic analysis." *IEEE Trans. on Power Systems*, **10:1**, pp. 433–440.

ARRILLAGA, J., N. R. WATSON, J. F. EGGLESTON, and C. D. CALLAGHAN (1987): "Comparison of steady-state and dynamic models for the calculation of AC/DC system harmonics." *IEE Proceedings*, **134C:1**, pp. 31–37.

ELECTRIC POWER RESEARCH INSTITUTE, INC. (EPRI), 3412 Hillview Avenue, Palo Alto, California 94304, USA (1989): *Electromagnetic Transients Program (EMTP) Revised Rule Book Version 2.0.*

FRIMAN, E. (1994): "Proposals for limits and responsibility sharing with regards to power quality." Technical Report. Swedish Transmission Research Institute, STRI AB, Box 707, s-77180 Ludvika, Sweden.

GILMORE, R. J. and M. B. STEER (1991): "Nonlinear circuit analysis using the method of harmonic balance – A review of the art. Part I. Introductory concepts." *Int J. Microwave and Millimeter-Wave Computer-Aided Eng.*, **1:1**, pp. 22–37.

HARRIS, F. J. (1978): "On the use of windows for harmonic analysis with the discrete fourier transform." *Proc. of the IEEE*, **66:1**, pp. 51–83.

IOTECH, INC., 25971 Cannon Road, Cleveland, Ohio 44146, USA (1995): *Daqbook/Daqboard/Daq – User's Manual.*

KEY, T. S. and J.-S. LAI (1993): "Comparison of standards and power supply design options for limiting harmonic distortion in power systems." *IEEE Trans. on Industry Applications*, **29:4**, pp. 688–695.

KUNDERT, K. S. and A. SANGIOVANNI-VINCENTELLI (1986): "Simulation of nonlinear circuits in the frequency domain." *IEEE Trans. on Computer-Aided Design*, **5:4**, pp. 521–535.

MATHWORKS, INC., 24 Prime Park Way, Natick, MA 01760-1500 (1996): *Signal Processing Toolbox User's Guide.*

MATTSSON, S. E., M. ANDERSSON, and K. J. ÅSTRÖM (1993): "Object-oriented modelling and simulation." In LINKENS, Ed., *CAD for Control Systems*, chapter 2, pp. 31–69. Marcel Dekker Inc, New York.

MOHAN, N., W. P. ROBBINS, T. M. UNDELAND, R. NILSSEN, and O. MO (1994): "Simulation of power electronic and motion control systems – an overview." *Proc. of the IEEE*, **82:8**, pp. 1287–1302.

OPPENHEIM, A. V. and R. W. SCHAFER (1989): *Discrete–Time Signal Processing.* Prentice–Hall, Inc., Englewood Cliffs, New Jersey.

RANADE, S. J. and W. XU (1998): *Tutorial on Harmonics Modeling and Simulation*, chapter 1. IEEE Power Engineering Society, IEEE Operations Center, P. O. Box 1331, 445 Hoes Lane, Piscataway, NJ 08855-1331 USA.

SEMLYEN, A., E. ACHA, and J. ARRILLAGA (1988): "Newton-type algorithms for the harmonic phasor analysis of non-linear power circuits in periodical steady state with special reference to magnetic non-linearities." *IEEE Trans. on Power Delivery*, **3:3**, pp. 1090–1098.

SEMLYEN, A. and N. RAJAKOVIĆ (1989): "Harmonic domain modeling of laminated iron core." *IEEE Trans. on Power Delivery*, **4:1**, pp. 382–390.

SONG, W., G. T. HEYDT, and W. M. GRADY (1984): "The integration of HVDC subsystems into the harmonic power flow algorithm." *IEEE Trans. on Power Apparatus and Systems*, **PAS-103:8**, pp. 1953–1961.

VLACH, J. and K. SINGHAL (1994): *Computer Methods for Circuit Analysis and Design*, second edition. Van Nostrand Reinhold, 115 Fifth Avenue, New York, NY 10003, USA.

XIA, D. and G. T. HEYDT (1982): "Harmonic power flow studies, Part I – Formulation and solution, Part II – Implementation and practical aspects." *IEEE Trans. on Power Apparatus and Systems*, **101:6**, pp. 1257–1270.

XU, W., J. E. DRAKOS, Y. MANSOUR, and A. CHANG (1994): "A three-phase converter model for harmonic analysis of HVDC systems." *IEEE Trans. on Power Delivery*, **9:3**, pp. 1724–1731.

XU, W., J. R. MARTI, and H. W. DOMMEL (1991): "A multiphase harmonic load flow solution technique." *IEEE Trans. on Power Systems*, **6:1**, pp. 174–182.

A

The Light Dimmer

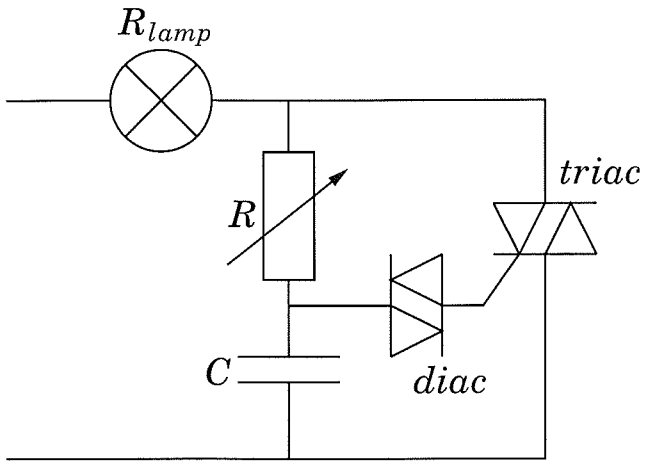

Figure A.1 A circuit diagram of a dimmer.

A dimmer is a device used to limit the power and thus dim the light from a light bulb. A circuit diagram of a dimmer is shown in Figure A.1. The basic component of a dimmer is a triac, a semiconductor device that works like two anti-parallel thyristors. The triac can conduct and block the current in either direction and is used to regulate AC current.

When the current through the triac crosses zero, it is turned off and blocks the current. The triac is turned on again by a gate signal. Typically, a gate current of 50 mA and a gate voltage of 1.5 V are required to turn on the triac.

The diac is, just like the triac, a symmetric switch. It is not controlled externally but starts to conduct when the voltage across it is $\pm$(20-40) V. The RC-circuit works as a timer. When the voltage across

the capacitor is high enough, the diac starts to conduct and signals the triac. The turn on time is adjusted with the variable resistor.

A.1 Analytical Calculation of the Equivalent for a Dimmer

The Harmonic Norton Equivalent is now derived for a dimmer, modelled as an ideal switch. If R_{lamp} is purely resistive, then after every zero-crossing of the voltage, the switch will be off for a time d. This means that the current through the dimmer is

$$i(t) = \begin{cases} 0, & t_0 < t < t_0 + d, \\ \frac{v(t)}{R_{lamp}}, & t_0 + d < t < t_1, \end{cases}$$

where t_0 and t_1 are two subsequent voltage zero-crossings. The dimmer is symmetric, that is, it behaves equally for negative and positive voltages. For a symmetric component, if the voltage is half-period anti-symmetric

$$v(t + \frac{T}{2}) = -v(t),$$

then so is the current. The Fourier series of signal that is half-period anti-symmetric contains only odd harmonics. For a network with only symmetric components, it is therefore sufficient to consider only the odd harmonics. Voltage and current are then written as

$$\begin{aligned} v(t) &= \sum_{k\,odd} a_k \cos k\omega_0 t + b_k \sin k\omega_0 t, \\ i(t) &= \sum_{k\,odd} A_k \cos k\omega_0 t + B_k \sin k\omega_0 t. \end{aligned} \tag{A.1}$$

At nominal voltage

$$v_0(t) = a_1^0 \cos \omega_0 t \quad \Longrightarrow \quad \begin{cases} a_1 = a_1^0, \\ a_k = a_k^0 = 0, & k > 1, \\ b_k = b_k^0 = 0, & k \geq 1, \end{cases} \tag{A.2}$$

there will be two zero-crossings per period. The time instants for these are obtained through

$$v(t^0) = a_1^0 \cos \omega_0 t^0 = 0 \qquad \Longrightarrow \qquad \omega_0 t^0 = \frac{\pi}{2} + n\pi.$$

Starting at $t = 0$, the first zero-crossing occurs at

$$t_1^0 = \frac{\pi}{2\omega_0}.$$

For small deviations from the nominal voltage

$$\begin{aligned} a_k &= a_k^0 + \widehat{a}_k, \\ b_k &= b_k^0 + \widehat{b}_k, \end{aligned}$$

there will still be two zero-crossings per period. The time for the first crossing is at

$$t_1 = t_1^0 + \widehat{t}_1,$$

where $\widehat{t}_1$ is small if $\widehat{a}_k$ and $\widehat{b}_k$ are small. Linearization gives

$$\begin{aligned} v(t_1) &= \sum_{k\,odd} a_k \cos k\omega_0 t_1 + b_k \sin k\omega_0 t_1 \\ &= \sum_{k\,odd} a_k \cos k\omega_0 (t_1^0 + \widehat{t}_1) + b_k \sin k\omega_0 (t_1^0 + \widehat{t}_1) \\ &= a_1^0(-\omega_0 \widehat{t}_1) + \sum_{k\,odd} \left(\widehat{b}_k (-1)^{\frac{k-1}{2}} + O(\widehat{a}_k^2 + \widehat{b}_k^2) \right) = 0, \end{aligned}$$

where it has been used that for $t_1^0 = \pi/2\omega_0$

$$\begin{aligned} \cos k\omega_0 t_1^0 &= \begin{cases} 0, & k \quad \text{odd}, \\ (-1)^{\frac{k}{2}}, & k \quad \text{even}, \end{cases} \\ \sin k\omega_0 t_1^0 &= \begin{cases} (-1)^{\frac{k-1}{2}}, & k \quad \text{odd}, \\ 0, & k \quad \text{even}. \end{cases} \end{aligned} \tag{A.3}$$

Neglecting higher order terms gives

$$\widehat{t}_1 = \frac{1}{\omega_0 a_1^0} \sum_{k\,odd} \widehat{b}_k (-1)^{\frac{k-1}{2}}. \tag{A.4}$$

The cosine coefficients for the current are obtained from the definition, utilizing the symmetry. For simplicity, R_{lamp} is set to 1.

$$\begin{aligned}
A_k &= \frac{2}{T}\int_0^T i(t)\cos k\omega_0 t\,dt = \frac{4}{T}\int_0^{T/2} i(t)\cos k\omega_0 t\,dt \\
&= \frac{4}{T}\left(\int_0^{T/2} v(t)\cos k\omega_0 t\,dt - \int_{t_1}^{t_1+d} v(t)\cos k\omega_0 t\,dt\right) \\
&= a_k - \frac{4}{T}\int_{t_1^0+\widehat{t}_1}^{t_1^0+\widehat{t}_1+d} \Big(a_1^0\cos\omega_0 t \\
&\quad + \sum_{l\,odd} \widehat{a}_l \cos l\omega_0 t + \widehat{b}_l \sin l\omega_0 t\Big)\cos k\omega_0 t\,dt \\
&= a_k^0 + \widehat{a}_k - \frac{4}{T}\int_{t_1^0}^{t_1^0+d} a_1^0\cos\omega_0 t\cos k\omega_0 t\,dt \\
&\quad + \frac{4}{T}\int_{t_1^0}^{t_1^0+\widehat{t}_1} a_1^0\cos\omega_0 t\cos k\omega_0 t\,dt \\
&\quad - \frac{4}{T}\int_{t_1^0+d}^{t_1^0+\widehat{t}_1+d} a_1^0\cos\omega_0 t\cos k\omega_0 t\,dt \\
&\quad - \frac{4}{T}\int_{t_1^0+\widehat{t}_1}^{t_1^0+\widehat{t}_1+d} \left(\sum_{l\,odd} \widehat{a}_l \cos l\omega_0 t + \widehat{b}_l \sin l\omega_0 t\right)\cos k\omega_0 t\,dt.
\end{aligned} \tag{A.5}$$

The terms in the last expressions can be linearized or simplified as

follows, using (A.4) and (A.3) and that $\omega_0 T = 2\pi$,

$$
\begin{aligned}
&a_k^0 - \frac{4}{T}\int_{t_1^0}^{t_1^0+d} a_1^0 \cos\omega_0 t \cos k\omega_0 t\, dt = A_k^0,\\
&\frac{4}{T}\int_{t_1^0}^{t_1^0+\widehat{t}_1} a_1^0 \cos\omega_0 t \cos k\omega_0 t\, dt = O(\widehat{t}_1^2),\\
&\frac{4}{T}\int_{t_1^0+d}^{t_1^0+d+\widehat{t}_1} a_1^0 \cos\omega_0 t \cos k\omega_0 t\, dt\\
&\quad = \frac{4}{T}\widehat{t}_1 a_1^0 \cos\omega_0(t_1^0+d)\cos k\omega_0(t_1^0+d) + O(\widehat{t}_1^2)\\
&\quad = \frac{2}{\pi}\sum_{l\,odd}\widehat{b}_l(-1)^{\frac{l-1}{2}}\sin\omega_0 d(-1)^{\frac{k-1}{2}}\sin k\omega_0 d + O(\widehat{t}_1^2),\\
&\frac{4}{T}\int_{t_1^0+\widehat{t}_1}^{t_1^0+\widehat{t}_1+d}\left(\sum_{l\,odd}\widehat{a}_l\cos l\omega_0 t + \widehat{b}_l\sin l\omega_0 t\right)\cos k\omega_0 t\, dt\\
&\quad = \frac{4}{T}\int_{t_1^0}^{t_1^0+d}\left(\sum_{l\,odd}\widehat{a}_l\cos l\omega_0 t + \widehat{b}_l\sin l\omega_0 t\right)\cos k\omega_0 t\, dt + O(\widehat{t}_1^2).
\end{aligned}
$$

Summarizing, this gives

$$
\begin{aligned}
A_k = A_k^0 + \widehat{a}_k + \frac{2}{\pi}\sum_{l\,odd}(-1)^{\frac{k+l}{2}}\widehat{b}_l\sin\omega_0 d\sin k\omega_0 d\\
- \frac{4}{T}\int_{t_1^0}^{t_1^0+d}\left(\sum_{l\,odd}\widehat{a}_l\cos l\omega_0 t + \widehat{b}_l\sin l\omega_0 t\right)\cos k\omega_0 t\, dt.
\end{aligned}
\tag{A.6}
$$

The sine coefficients are obtained in the same way as

$$
\begin{aligned}
B_k = B_k^0 + \widehat{b}_k - \frac{2}{\pi}\sum_{l\,odd}(-1)^{\frac{k+l}{2}}\widehat{b}_l\sin\omega_0 d\cos k\omega_0 d\\
- \frac{4}{T}\int_{t_1^0}^{t_1^0+d}\left(\sum_{l\,odd}\widehat{a}_l\cos l\omega_0 t + \widehat{b}_l\sin l\omega_0 t\right)\sin k\omega_0 t\, dt.
\end{aligned}
\tag{A.7}
$$

The elements in Y are the partial derivatives of the Fourier coefficients of the current (A.6) and (A.7)

$$\begin{aligned}
\frac{\partial A_k}{\partial a_l} &= \delta_{kl} - \frac{4}{T}\int_{t_1^0}^{t_1^0+d} \cos l\omega_0 t \cos k\omega_0 t\, dt, \\
\frac{\partial A_k}{\partial b_l} &= \frac{2}{\pi}(-1)^{\frac{k+l}{2}} \sin \omega_0 d \sin k\omega_0 d \\
&\quad - \frac{4}{T}\int_{t_1^0}^{t_1^0+d} \sin l\omega_0 t \cos k\omega_0 t\, dt, \\
\frac{\partial B_k}{\partial a_l} &= -\frac{4}{T}\int_{t_1^0}^{t_1^0+d} \cos l\omega_0 t \cos k\omega_0 t\, dt, \\
\frac{\partial B_k}{\partial b_l} &= \delta_{kl} - \frac{2}{\pi}(-1)^{\frac{k+l}{2}} \sin \omega_0 d \cos k\omega_0 d \\
&\quad - \frac{4}{T}\int_{t_1^0}^{t_1^0+d} \sin l\omega_0 t \sin k\omega_0 t\, dt.
\end{aligned} \tag{A.8}$$

To obtain analytical expressions for I_0 and Y, the integrals in (A.6), (A.7) and (A.8) must be derived analytically. Using trigonometric relations this means that the following integrals must be solved, with $m = l + k$ or $m = l - k$.

$$\begin{aligned}
\int_{t_1^0}^{t_1^0+d} \cos m\omega_0 t\, dt &= \frac{1}{m\omega_0}[\sin m\omega_0 t]_{t_1^0}^{t_1^0+d} = \frac{(-1)^{m/2}}{m\omega_0} \sin m\omega_0 d, \\
\int_{t_1^0}^{t_1^0+d} \sin m\omega_0 t\, dt &= \frac{1}{m\omega_0}[-\cos m\omega_0 t]_{t_1^0}^{t_1^0+d} = \frac{(-1)^{m/2}}{m\omega_0}(1 - \cos m\omega_0 d),
\end{aligned} \tag{A.9}$$

where $m \neq 0$. For $m = 0$ the integrals become

$$\begin{aligned}
\int_{t_1^0}^{t_1^0+d} \cos m\omega_0 t\, dt &= \int_{t_1^0}^{t_1^0+d} 1\, dt = d, \\
\int_{t_1^0}^{t_1^0+d} \sin m\omega_0 t\, dt &= \int_{t_1^0}^{t_1^0+d} 0\, dt = 0.
\end{aligned} \tag{A.10}$$

The elements of I_0 are obtained from (A.6) and (A.7) using (A.9) and (A.10). For $k = 1$

$$A_1^0 = a_1^0 - \frac{2a_1^0}{\pi}\left(-\frac{1}{2}\sin 2\omega_0 d + \omega_0 d\right),$$
$$B_1^0 = -\frac{2a_1^0}{\pi}\frac{1}{2}(1 - \cos 2\omega_0 d),$$

and for odd $k > 1$

$$A_k^0 = -\frac{2a_1^0}{\pi}\left(\frac{(-1)^{\frac{k+1}{2}}}{k+1}\sin(k+1)\omega_0 d + \frac{(-1)^{\frac{k-1}{2}}}{k-1}\sin(k-1)\omega_0 d\right),$$
$$B_k^0 = -\frac{2a_1^0}{\pi}\left(\frac{(-1)^{\frac{k+1}{2}}}{k+1}(1 - \cos(k+1)\omega_0 d) + \frac{(-1)^{\frac{k-1}{2}}}{k-1}(1 - \cos(k-1)\omega_0 d)\right).$$

The elements in Y, with $m = l+k$, $n = l-k$, and $R_{lamp} = 1$, become for $n = 0$

$$\frac{\partial A_k}{\partial a_k} = \frac{1}{\pi}\left(\pi - \frac{(-1)^{m/2}}{m}\sin m\omega_0 d - \omega_0 d\right),$$
$$\frac{\partial A_k}{\partial b_k} = \frac{1}{\pi}\left(-\frac{(-1)^{m/2}}{m}(1 - \cos m\omega_0 d + 2\sin\omega_0 d \sin k\omega_0 d)\right),$$
$$\frac{\partial B_k}{\partial a_k} = \frac{1}{\pi}\left(-\frac{(-1)^{m/2}}{m}(1 - \cos m\omega_0 d)\right),$$
$$\frac{\partial B_k}{\partial b_l} = \frac{1}{\pi}\left(\pi + \frac{(-1)^{m/2}}{m}(\sin m\omega_0 d + 2\sin\omega_0 d \cos k\omega_0 d) - \omega_0 d\right),$$

and for $n \neq 0$

$$\frac{\partial A_k}{\partial a_l} = \frac{1}{\pi}\left(-\frac{(-1)^{m/2}}{m}\sin m\omega_0 d - \frac{(-1)^{n/2}}{n}\sin n\omega_0 d\right),$$

$$\frac{\partial A_k}{\partial b_l} = \frac{1}{\pi}\left(-\frac{(-1)^{m/2}}{m}(1-\cos m\omega_0 d + 2\sin\omega_0 d \sin k\omega_0 d)\right.$$
$$\left.-\frac{(-1)^{n/2}}{n}(1-\cos n\omega_0 d)\right),$$

$$\frac{\partial B_k}{\partial a_l} = \frac{1}{\pi}\left(-\frac{(-1)^{m/2}}{m}(1-\cos m\omega_0 d) + \frac{(-1)^{n/2}}{n}(1-\cos n\omega_0 d)\right),$$

$$\frac{\partial B_k}{\partial b_l} = \frac{1}{\pi}\left(\frac{(-1)^{m/2}}{m}(\sin m\omega_0 d + 2\sin\omega_0 d\cos k\omega_0 d)\right.$$
$$\left.-\frac{(-1)^{n/2}}{n}\sin n\omega_0 d\right).$$

The Harmonic Norton Equivalent for $R_{lamp} \neq 1$ is obtained by dividing Y and I_0 by R_{lamp}.

To show some numerical values, the Norton Equivalent for the dimmer used in Section 3.2 is presented. It is linearized around the nominal voltage

$$v_0(t) = 230\sqrt{2}\cos\omega_0 t,$$

with

$$\omega_0 = 2\pi 50,$$
$$d = \frac{1}{6}T.$$

The harmonics up to order 7 are shown.

$$I_0 = \frac{1}{R_{lamp}} \begin{bmatrix} 273.530 & 81.169 & 70.294 & 40.585 & 23.431 & -40.585 & -11.716 & -20.292 \end{bmatrix},$$

$$Y = \frac{1}{R_{lamp}} \begin{bmatrix} 0.804 & -0.239 & 0.207 & 0.597 & 0.069 & -0.597 & -0.034 & 0.418 \\ 0.239 & 0.804 & -0.358 & -0.207 & 0.119 & 0.345 & -0.060 & -0.241 \\ 0.207 & -0.358 & 0.667 & 0 & 0.103 & 0.179 & 0.041 & -0.0712 \\ 0.119 & 0.620 & 0 & 0.115 & -0.298 & 0.724 & 0.167 & -0.455 \\ 0.069 & 0.597 & 0.103 & -0.776 & 0.639 & 0.525 & 0.138 & -0.239 \\ -0.119 & 0.345 & 0.179 & -0.103 & 0.048 & 0.970 & -0.239 & -0.138 \\ -0.034 & 0.418 & 0.041 & -0.310 & 0.138 & 0.239 & 0.686 & -0.443 \\ -0.060 & -0.241 & -0.072 & 0.372 & 0.239 & -0.138 & 0.034 & 0.923 \end{bmatrix},$$

$$I_E = YV_0 - I_0 = \begin{bmatrix} 0 & 0 & 0 & 0 & 0 & 0 & 0 & 0 & 0 & 0 & 0 & 0 \end{bmatrix}.$$

The reason why $I_E = 0$ is that for an undistorted voltage, the current is proportional to the voltage amplitude. Thus, I_0 is proportional to the first column of Y. This is, however, not true for all power electronic components.

B

Standards on Harmonics Limits

The interconnection of networks owned by different companies, and the deregulation of the power market, implies that there is a need for rules on how the responsibility for keeping the distortion within acceptable limits is shared between power producers, network owners, distributors, and consumers. To get to grips with the problem of increasing distortion, organizations like IEEE and IEC have come up with standards that limit the allowed distortion level.

To quantify the harmonic distortion of the power, the standards use two definitions, relative harmonics content, and total harmonic distortion. The relative harmonics content, RHC, is the effective value of one harmonic divided by the effective value of the fundamental harmonic

$$RHC_v = \frac{V_n}{V_1}, \qquad RHC_i = \frac{I_n}{I_1},$$

for voltage and current respectively.

The total harmonic distortion, THD, is sometimes also called the total relative harmonics content. It is derived as the square root of the quadratic sum of the relative harmonics content for all harmonic frequencies. For the voltage this gives

$$THD_v = \sqrt{\sum_{n=2}^{\infty} \left(\frac{V_n}{V_1}\right)^2}.$$

System Voltage		RHC (%) Odd harmonics no.						
		3–9	11	13	15–17	19	21–25	>25
LV	< 1kV	4	3.5	3	2	1.5	1.5	$0.2 + 1.3\frac{25}{n}$
MV	< 40kV	3	2.5	2	1.5	1	1	$0.2 + 0.8\frac{25}{n}$
HV	≥ 40kV	1	1	1	1	1	0.7	$0.2 + 0.5\frac{25}{n}$

		RHC (%) Even harmonics no.				THD (%)
		2–4	6	8–10	>10	
LV	<1kV	1	0.5	0.5	0.2	6.0
MV	<40kV	1	0.5	0.2	0.2	4.5
HV	≥40kV	0.5	0.5	0.2	0.2	1.5

Table B.1 Target limits for voltage harmonics in the Swedish power network, according to STRI.

System Voltage		RHC (%) Harmonics no.		THD (%)
		$n \leq 13$	$n > 13$	
LV	< 1kV	6	3	7
MV	< 40kV	6	3	7
HV	≥ 40kV	4	2	5

Table B.2 Target limits for current harmonics in the Swedish power network, according to STRI.

In a proposal, [Friman, 1994], STRI (the Swedish Transition Research Institute) have come up with limits on the voltage and current harmonics. These are almost identical to other organizations standards, only adjusted to fit to Swedish conditions. The distortion limits are gathered in Tables B.1, and B.2.

The distortion of the voltage is normally not that severe. For the current it is much worse. In office buildings, where computers, air conditioning and low energy lighting dominates the loads, 40% THD in the current is not unusual, [Key and Lai, 1993].